Dynamics of Global Emission Permit Prices and Regional Social Cost of Carbon under Noncooperation *

Yongyang Cai† Khyati Malik‡ Hyeseon Shin§

November 4, 2025

Abstract

We build a dynamic multi-region model of climate and economy with emission permit trading among 12 aggregated regions of the world. We solve for the dynamic Nash equilibrium under noncooperation, wherein each region adheres to the emission cap constraints following commitments that were first outlined in the 2015 Paris Agreement and later strengthened under the Glasgow Pact. Our model shows that the emission permit price reaches $923 per ton of carbon by 2050, and global average temperature is expected to reach 1.7 degrees Celsius above the pre-industrial level by the end of this century. We demonstrate, both theoretically and numerically, that the regional social cost of carbon is equal to the difference between the regional marginal abatement cost and the permit price, illustrating complementarity between emission trading system and carbon tax. That is, heterogeneity in social cost of carbon across regions

*The authors have contributed equally to this work. We are grateful for comments and suggestions from the participants at PACE 2023, the Heartland Environmental and Resource Economics Workshop 2023, OSU Interdisciplinary Research Fall Forum: Computational Approaches for a Just and Sustainable World 2023, the LSE Environment Camp 2024, the 2nd China Energy Modeling Youth Forum, Tokyo Workshop of Climate Finance & Risk 2024, Climate Change Economics Forum, and seminars at University of Illinois Urbana-Champaign, Beijing Institute of Technology, University of Chinese Academy of Sciences, Ohio University, and Peking University. Cai acknowledges support from the National Science Foundation grant SES-1739909 and the USDA-NIFA-AFRI grant 2018-68002-27932. Malik acknowledges funding from the USDA postdoctoral fellowship "New Perspectives on Agricultural Economics" awarded through the National Bureau of Economic Research. Shin acknowledges the support from the endowments of The Andersons Program in International Trade and the Sogang University Research Grant 202510015.01.

†Department of Agricultural, Environmental and Development Economics, The Ohio State University. cai.619@osu.edu

‡National Bureau of Economic Research (NBER). malikk@nber.org

§Corresponding author. Department of Economics, Sogang University. hsshin@sogang.ac.kr

implies that a uniform global carbon price alone may not achieve regionally optimal carbon pricing. We find significant heterogeneity in the regional social cost of carbon, and that global emission trading has little impact on this measure. We also find that when the regional emission caps are lax, and therefore non-binding, a global emission trading system may lead to higher emissions under noncooperation, underscoring the necessity of maintaining stringent global emission caps to ensure efficient functioning of the emission trading system. Finally, simulations of a partial emission trading system, where one major region opts out, highlight pronounced free-rider incentives and the persistent challenge of sustaining global cooperation on carbon mitigation.

Keywords: Emission trading system, Paris Agreement, dynamic Nash equilibrium, integrated assessment model, carbon tax, social cost of carbon.

JEL Classification: C73, F18, Q54, Q58.

1 Introduction

Climate change has raised concerns of disastrous consequences, ranging from rising sea levels to increase in the frequency and intensity of extreme weather events (Arias et al., 2021). International efforts to address climate change have evolved over the past three decades, commencing with the United Nations Framework Convention on Climate Change (UNFCCC) in 1992, followed by the Kyoto Protocol in 1997, the Paris Agreement in 2015, and the Glasgow Pact in 2021. The policy outlined in the Paris Agreement codified an objective of "limiting global average temperature rise to well below 2 degrees Celsius above pre-industrial levels, with a pursuit of limiting it to 1.5 degrees Celsius" (Article 2). To accomplish this objective, 194 countries (regions) committed to the Nationally Determined Contributions (NDCs), which specify their emission mitigation goals. The Glasgow Climate Pact, adopted at the UN Climate Change Conference in Glasgow (COP26) in November 2021, revisited the NDCs, reaffirming the previous commitments made in the Paris Agreement and recognizing the need for more stringent efforts to attain the global target of 1.5 degrees Celsius.

Various market-based approaches have been proposed to reduce emissions, among which carbon tax regimes and emission trading systems (ETSs) are the most prominent.[1] In a carbon tax regime, a tax is charged to firms for each unit of carbon emission. Previous studies have argued that the optimal global carbon tax rate is equal to the global social cost of carbon (SCC), which is the present value of global climate damages incurred by an additional unit of atmospheric carbon emissions (Nordhaus, 2017). In an emission trading or a cap-and-trade system, on the other hand, the maximum amount of permissible emissions is fixed in an economy, and agents can sell and purchase emission permits (allowances) at market-determined prices. In the absence of transaction costs and uncertainty, properly designed carbon tax and emission trading regimes are argued to yield equivalent outcomes in several key aspects (e.g., incentives for emission reductions, aggregate abatement costs, and carbon leakage) (Montgomery, 1972; Goulder and Schein, 2013; Stavins, 2022). In 2005, the European Union (EU) first adopted a legally binding emission trading system among the EU members,[2] and as of the winter of 2024, the permit price stands at about 70 euros per ton of Carbon Dioxide (CO_2).[3]

In this study, we develop and quantify a dynamic multi-region model of the climate and

[1] It has been documented that a total of 61 carbon pricing policies, consisting of 30 taxes and 31 ETSs, have been executed or are scheduled for implementation globally (Stavins, 2022).

[2] In addition to the EU ETS, other national or sub-national ETSs have been implemented or are in the process of development, including in Canada, China, Japan, New Zealand, South Korea, Switzerland, and the United States. For information on the most up-to-date policy in practice, see World Bank Carbon Pricing Dashboard (https://carbonpricingdashboard.worldbank.org/).

[3] Source of EU permit price: (https://tradingeconomics.com/commodity/carbon).

economy under an emission trading system (ETS), while the ETS could be global or partial. The model framework extends the seminal Regional Integrated Model of Climate and the Economy (RICE) (Nordhaus and Yang, 1996; Nordhaus, 2010b), which captures the interactions between economic growth and climate systems in a multi-regional framework. As in the standard neoclassical growth model (the so-called Ramsey model), a social planner of each region chooses investment in capital goods to smoothen consumption over time. Economic activity generates both output and carbon emissions; the latter induces climate damages that endogenously reduce regional output. Emission abatement efforts can reduce carbon emissions but are costly. As emissions generate global externalities, each region has less incentive to undertake abatement on its own while benefiting from the abatement efforts of others. In a noncooperative environment, a set of the optimal strategies of each regional social planner, involving dynamic choices over consumption and emission abatement, is characterized as a Nash equilibrium concept from game theory (Nordhaus and Yang, 1996). The introduction of the ETS imposes exogenous region-specific emissions caps and allows permit trading across regions. Under the ETS, regional social planners jointly determine the optimal paths of consumption, emission abatement, and the amount of permit trading, subject to strictly-enforced emission cap constraints. Heterogeneity across regions, in abatement technologies, climate damages, productivity, carbon intensity, and emissions cap constraints, causes divergence in regional marginal abatement costs (MAC) and the regional social cost of carbon across regions, shaping the path of the market equilibrium permit price over time.

In an ETS scheme, the primary forces that shape the equilibrium outcome include regional climate damages, revenues or costs from permit trading, and regional abatement costs. Using a simple static framework where a regional social planner i internalizes climate damages and chooses optimal net emissions, E_i, (i.e., emissions after abatement), we show that the equilibrium condition for optimal abatement can be expressed as: $\text{SCC} = \text{MAC}(E_i) - m$, where m is the market price of emission permits. This relationship between regional SCC, MAC, and emission price has an important implication: a positive regional SCC implies $\text{MAC}(E_i) > m$, suggesting that a region experiencing climate damages has an incentive to abate emissions up to a level where the MAC exceeds the market price of emission permits. We emphasize that this equilibrium condition represents the necessary condition for achieving the optimal level of net emissions *from the perspective of each regional social planner*.

In the literature, the equality between MAC and permit price is used as a competitive equilibrium condition under an ETS regime *in a decentralized economy*, where individual firms internalize the emission price. This condition is derived from the perspective of individual firms in the ETS when they face no additional carbon tax. If a carbon tax τ_i is levied on firms on top of the permit price, the competitive equilibrium condition becomes

$\tau_i = \text{MAC}(E_i') - m'$ in the decentralized economy, where E_i' and m' are the corresponding net emissions and permit price under the decentralized equilibrium with tax τ_i. If the carbon tax is set equal to the regional SCC in each region, then E_i' and m' are equal to the regional social planner's optimal net emissions and permit price. Moreover, because climate damages—and hence the regional SCC—differ across regions, a uniform global carbon price alone may not achieve regionally optimal level of emission pricing. The appropriate equilibrium condition in this context, $\text{SCC} = \text{MAC}(E_i) - m$, further implies that carbon taxation and cap-and-trade are not competing instruments but rather complementary.

We bring the model to data by aggregating 152 countries into 12 world regions and simulating the model at annual time steps. The model is calibrated by fitting it to historical data and the recent predicted trends of regional climate damage (Burke et al., 2018), regional total factor productivity (Burke et al., 2018), regional abatement costs (Ueckerdt et al., 2019), and population projections based on the Shared Socioeconomic Pathway 2 (SSP2; Samir and Lutz, 2017), also known as the "Middle-of-the-Road" scenario. Besides this calibration, our model uses a stylized but stable climate system, called the Transient Climate Response to Emissions (TCRE; Matthews et al., 2009), which assumes that increases in the global averaged atmospheric temperature have a nearly linear functional dependence on the cumulative carbon emissions. We demonstrate that this temperature system can be calibrated to match closely with the various Representative Concentration Pathways (RCPs; Meinshausen et al., 2011). Due to its simplicity and effectiveness, the TCRE scheme has found applications in recent economic analyses, as evidenced by studies such as Brock and Xepapadeas (2017), Dietz and Venmans (2019), Mattauch et al. (2020), and Barnett et al. (2020). Additionally, Dietz et al. (2021) show that the TCRE scheme does not lead to a large difference in economic analysis with the seminal DICE framework (Nordhaus, 2017), compared to other more complicated climate systems.

For regional emission cap scenarios, we construct emission cap pathways reflecting the latest emission targets for 2030 and net-zero pledges for 2050-2070, contributing to the scant literature on evaluating the economic and environmental implications of these commitments (e.g., van de Ven et al., 2023; Meinshausen et al., 2022; den Elzen et al., 2022). For each region, emissions cap trajectories are constructed to align with the latest nationally determined contributions (NDCs) under the Paris Agreement and the Glasgow Climate Pact. These trajectories reflect near-term targets for 2025 and 2030, as well as long-term net-zero commitments spanning 2050 to 2070, and are treated as exogenous constraints.

Our numerical simulations, based on newly calibrated parameters, provide comprehensive results on the potential economic and environmental outcomes under the ETS. Assuming

full compliance with these emission caps and no future revisions,[4] the emission permit price is endogenously determined by annual supply and demand in the global permit market. Under the baseline emission cap scenario based on the Paris Agreement and Glasgow Pact commitments, our simulation results show that the oversupply of global permits in the initial years results in zero permit prices, but by 2050, the emission permit price can reach up to $923 per ton of carbon. The corresponding global average temperature is expected to reach 1.7 degree Celsius above the pre-industrial level by the end of this century. Furthermore, our simulation results numerically confirm that the regional SCC exactly equals the difference between the regional MAC and the permit price, as explored in the predictions of the static framework. For instance, in 2050, the MAC for the United States is estimated at $1,159 per ton of carbon, the permit price at $923, and the resulting difference of $236 matches the regional SCC calculated independently from the model.

A comparative analysis of the roles of emission caps and the ETS further illustrates several key findings. First, the findings indicate that the ETS with the baseline emission caps leads to higher emissions under noncooperation, as regions with binding emission caps can purchase permits from less constrained regions, exploiting the surplus permits in the initial years. This highlights the necessity of maintaining stringent global emission caps to ensure the efficient functioning of the ETS. Second, our welfare analysis reveals that when the global emission cap is sufficiently tight, the ETS can lead to welfare improvements for all participating regions. These welfare improvements reflect efficiency gains achieved by reallocating abatement efforts across regions through market mechanisms.

Additionally, leveraging the flexibility of our model, we evaluate two additional set of policy scenarios, including a partial ETS participation and alternative emission caps consistent with different net-zero targets. Recognizing the challenges of achieving international cooperation on climate policies, we consider a scenario in which one major region (the United States) opts out of the global cap-and-trade system. The results show that the United States experiences a notable welfare gain. This outcome underscores strong free-rider incentives, as the opt-out region faces a lighter abatement burden while benefiting from the emission reductions undertaken by participating regions. In a second policy experiment, we find that tightening the global emission cap leads to higher permit prices across future periods. For instance, if all regions achieve net-zero emissions by 2050, the permit price could reach $1,621

[4]This paper assumes that regions do not revise their NDC limits (emission cap constraints) in the future. While primarily introduced to address computational challenges, this assumption is also supported by economic and institutional considerations: (i) relaxing NDC limits could result in penalties from other regions or damage to the region's reputation; (ii) reducing NDC limits would lead to a loss of benefits from selling emission permits or more cost from purchasing; and (iii) renegotiating NDC limits is often time-consuming and infrequent.

per ton of carbon by 2049. However, even with such strict emissions restrictions, the global temperature is projected to rise by 1.62°C by the end of the century. These results suggest that meeting the global target of limiting warming to 1.5°C will require even more stringent emission reduction commitments than those set out in the Glasgow Pact, albeit at the cost of significantly higher permit prices. Our results are qualitatively consistent with the findings of other IAMs (van de Ven et al., 2023; Meinshausen et al., 2022; den Elzen et al., 2022), which indicate that the strengthened post-Glasgow NDC and net-zero targets, covering both near-term and long-term goals, are insufficient to limit warming to 1.5°C above the pre-industrial level, though full implementation could restrict warming to below 2°C. Finally, to ensure the robustness of our results, we conduct sensitivity analyses using alternative parameter values for climate damages and abatement costs, calibrated to empirical estimates reported in the key existing literature.

2 Related Literature

This paper contributes to the literature on macroeconomic modeling of climate change. Our model framework is closely related to the RICE model (Nordhaus and Yang, 1996; Nordhaus, 2010b; Yang, 2023), an extension of the global DICE model (Nordhaus, 2014) in a multi-region framework, capturing interactions between economic growth and climate systems. However, Nordhaus and Yang (1996) and Yang (2023) do not investigate an ETS, and Nordhaus (2010b) does not solve a problem with an ETS under noncooperation. Following the RICE model, a group of studies have explored climate policy in a dynamic multi-regional framework under cooperation and noncooperation. For instance, Luderer et al. (2012) and Jakob et al. (2012) compare the long-term predictions of three-region energy-economy models under specific environmental targets, such as stabilizing the atmospheric CO_2 concentrations at 450 ppm. However, these studies do not incorporate actual NDCs or regional net-zero targets to assess the region-specific emissions and economic pathways. Other studies, such as van der Ploeg and de Zeeuw (2016) and Jaakkola and Van der Ploeg (2019), focus on stochastic events, including climate tipping points and technological breakthroughs, comparing the results under different levels of cooperation. Cai et al. (2023) build a dynamic IAM for two economic regions (North and Tropic/South) to compute regional SCCs under cooperation and noncooperation. Hambel et al. (2021) extend the RICE framework by integrating endogenous international trade under noncooperation and provide a closed-form analytical solution for the regional SCCs under certain model assumptions. Iverson and Karp (2021) study a Markov perfect equilibrium in a dynamic game with a social planner deciding climate policies and non-constant discount rates. For a comprehensive review of

macroeconomic models of climate change, see Fernández-Villaverde et al. (2025). Nonetheless, the literature has yet to examine the dynamics of an ETS with an endogenous market price of emission permits and regional SCCs under a noncooperative setting. This paper addresses this gap by providing a comprehensive analysis of an ETS as well as identifying the relationship between permit prices and regional SCCs under a multi-region dynamic noncooperative framework.

This paper also adds to the extensive literature on environmental economic policy, with a particular focus on carbon pricing. ETSs, alongside carbon taxes, have garnered attention as promising mechanisms for reducing global emissions. However, comprehensive analyses of ETSs as instruments for global climate policy remain relatively limited. Among the most closely related studies are extensions of the WITCH model (Bosetti et al., 2006) that incorporate an ETS, including the analyses of regional ETSs for Asian countries (Massetti and Tavoni, 2012), endogenous technological change (De Cian and Tavoni, 2012), and banking of emission permits (Bosetti et al., 2009). The WITCH model considers alternative emission permit allocation schemes in which permits are distributed according to population or current emission shares, whereas our study applies emission caps consistent with the Paris Agreement and the Glasgow Climate Pact. In addition, our study departs from previous WITCH analyses by examining regional SCCs and their economic policy implications under an ETS, which were not explored in earlier studies. Carbone et al. (2009) present another relevant study, constructing a computable general equilibrium model incorporating countries' endogenous participation in an ETS and allocation of emission permits, and solving for the equilibrium permit price. Yet, Carbone et al. (2009) examine the ETS in a static setting, missing the crucial dynamic aspects of climate change and its connection with emission abatement decisions. Fischer and Springborn (2011) develop a dynamic stochastic general equilibrium model to compare outcomes of emission caps and tax policies, but they do not allow for emission trading between regions. Another group of studies examines the potential efficiency gains from integrating regional ETSs into a global system (Habla and Winkler, 2018; Doda et al., 2019; Holtsmark and Weitzman, 2020; Holtsmark and Midttømme, 2021; Mehling et al., 2018). Some studies highlight that differentiated emission pricing under ETSs based on location-specific damages can be welfare improving (Muller and Mendelsohn, 2009; Holland and Yates, 2015; Fowlie and Muller, 2019).

More broadly, a substantial body of literature has examined ETSs from various perspectives. Several studies have analyzed how the initial allocation of permits affects the equilibrium outcomes (Hahn and Stavins, 2011), or have compared allocation methods between auctioning and free allocation (Goulder and Parry, 2008; Goulder et al., 2010). Other studies have compared the relative efficiency of carbon policies under cost uncertainty, show-

ing that carbon tax can be more efficient than ETS under certain conditions, and vice versa (Weitzman, 1974; Stavins, 1996; Karp and Traeger, 2024). In another strand of literature, a number of studies have focused on empirically analyzing the regional emission trading markets currently in practice, such as the EU ETS (Hitzemann and Uhrig-Homburg, 2018; Fuss et al., 2018; Perino et al., 2022), China ETS (Goulder et al., 2022), or California ETS (Borenstein et al., 2019). An important issue with a regional ETS is carbon leakage, which refers to the shift of emission intensive production to regions outside the jurisdiction of the ETS. Previous studies have compared different policy instruments aimed at mitigating this problem and providing a level-playing field to the firms operating within the ETS (Ambec et al., 2024; Böhringer et al., 2014; Farrokhi and Lashkaripour, 2021; Fowlie and Reguant, 2022; Levinson, 2023).

While there is no general agreement among economists on whether carbon taxation or ETS is better (Stavins, 2022), previous works have often considered these two pricing instruments (trading versus taxes) as policy substitutes. For instance, some studies support carbon taxation over ETS, highlighting concerns about price volatility in ETS (Nordhaus, 2007), or the presence of uncertainty regarding emission abatement costs (Newell and Pizer, 2003). For instance, Newell and Pizer (2003) find that carbon taxation can yield higher welfare benefits than ETS under such uncertainties. Conversely, other studies advocate ETS over carbon taxation because allocation of permits in ETS allows for more flexibility, and ETS faces less uncertainty in controlling the cumulative amount of carbon emissions compared to taxes (Keohane, 2009). Harstad and Eskeland (2010), Hahn and Stavins (2011), and Stavins (2022) argue that from a practical perspective, ETS may be a preferred instrument over tax, as free allowances could be negotiated among participating agents to redistribute burden and, thus be used to gain political support. Moreover, in a global ETS, emission permits will be traded globally with one price for all nations based on market forces, which may alleviate the problem of carbon leakage (Fowlie et al., 2016). However, Harstad and Eskeland (2010) argue that although an ETS in a perfect market is the first-best system, frequent government interventions to redistribute allocations among firms may result in distortions in the market allocation.[5] For a comprehensive comparison on carbon taxation and trading regimes, see e.g., Strand (2013); Schmalensee and Stavins (2017); Cai (2021); Stavins (2022). This study contributes to the literature by showing that regional carbon tax is complementary to ETS under noncooperation.

[5]Environmental pollution has also been studied from the context of fiscal federalism, which considers what level of government should regulate pollution (Oates, 1999; Ogawa and Wildasin, 2009; Banzhaf and Chupp, 2012; Williams III, 2012).

3 A Static Framework of Climate and the Economy with an ETS

This section presents a simplified static model framework with a global ETS to provide intuition on the relationship between the regional SCC and regional MAC. In a global ETS regime, the main forces determining the equilibrium are climate damages, costs (or revenue) from emissions trading, and costs from regional emission abatement efforts. In this simplified static framework, it can be easily shown that the regional SCC equals the regional MAC minus the market price of emission permits. Building on these insights, the next section presents the multi-region dynamic general equilibrium model, followed by the quantification strategies and numerical analysis.

Consider a world economy with multiple regions under a global ETS regime, and let $\mathcal{I}$ denote the set of regions. Each region $i \in \mathcal{I}$ is allocated an exogenous emission cap $\bar{E}_i$, which represents the region's maximum allowable emissions and is strictly enforced. Economic activity generates emissions, with E_i^{Gross} denoting a region's *gross emissions*, which are treated as exogenous in this simplified framework.[6] To comply with the emission cap constraint, each region's social planner can either (i) purchase or sell emission permits in the global emission market, or (ii) undertake costly abatement efforts. Let E_i denote its *emissions net of abatement* (henceforth referred to as *net emissions*), and E_i^P the quantity of *emission permits purchased* in the market. A positive E_i^P indicates that the region purchases permits, while a negative E_i^P indicates that the region sells permits. The emission cap constraint for each region is then given by $E_i \leq \overline{E}_i + E_i^P$.

In this economy, the regional social planner aims to minimize the total economic costs associated with its emissions, including (i) climate damages due to global emissions, (ii) costs (or revenue) from emission trading, (iii) and costs from own regional emission abatement. Formally, a social planner of each region solves the following minimization problem:

$$\min_{0 \leq E_i \leq \overline{E}_i + E_i^P} \underbrace{D_i\left(\sum_{j \in \mathcal{I}} E_j\right)}_{\text{Climate Damages}} + \underbrace{mE_i^P}_{\text{ETS Costs/Revenue}} + \underbrace{\int_{E_i}^{E_i^{\text{Gross}}} \text{MAC}_i(E)dE}_{\text{Emission Abatement Cost}}. \tag{1}$$

The first term of the objective function represents regional climate damages, where $D_i(\cdot)$ is a function that captures the regional climate damages from global net emissions, $\sum_{j \in \mathcal{I}} E_j$.

[6] It is innocuous to assume that gross emissions are exogenous in this static framework. In the full dynamic model introduced later, regional gross emissions are proportional to GDP, which is determined by capital and the exogenous population growth. Given that the current level of capital is determined in the previous period, gross emissions can be considered exogenous for each period in a static equilibrium.

Here $D_i(\cdot)$ can also be considered as the present value of future climate damages from the current global net emissions in the corresponding dynamic framework. The second term accounts for the cost (or revenue) from purchasing (or selling) permits at price m, which is the Nash equilibrium price satisfying the market clearing condition $\sum_{j\in\mathcal{I}} E_j^P = 0$. The quantity of emission permits purchased may influence the global permit price, making the market price depend on their emission permit purchase choices, which in turn are contingent on the trade decisions of other regions. Lastly, the third term reflects the total abatement cost incurred to reduce emissions by $(E_i^{\text{Gross}} - E_i)$, where $\text{MAC}_i(\cdot)$ denotes the region's marginal abatement cost and is assumed to be monotonically increasing over E_i, with $\text{MAC}_i(E_i^{\text{Gross}}) = 0$. For simplicity, it is assumed that net emissions are nonnegative throughout the paper.[7]

In the static Nash equilibrium of the world economy, every regional social planner simultaneously solves equation (1) while satisfying the market-clearing condition $\sum_{j\in\mathcal{I}} E_j^P = 0$, which implies that $\sum_{j\in\mathcal{I}} E_j \leq \sum_{j\in\mathcal{I}} \overline{E}_j$. We assume that each region is a price taker for permits, as a large number of firms in each region participate in the permit trading market in practice. Thus, the Karush-Kuhn-Tucker conditions of equation (1) imply that the solution to the region's optimal net emissions leads to the following relationship between the marginal regional damage, the MAC, and the permit price:

$$\underbrace{\frac{\partial D_i(\sum_{j\in\mathcal{I}} E_j)}{\partial E_i}}_{\text{Regional SCC}} = \underbrace{\text{MAC}_i(E_i) - m}_{\text{Deviation from Market Equilibrium}}, \tag{2}$$

when $E_i > 0$. The left hand side of this equation represents the marginal regional damage, which corresponds to the regional SCC. This term captures the additional regional economic cost imposed by a unit increase in global emissions, reflecting the region's contribution to global climate change. The right hand side captures the difference between $\text{MAC}_i(E_i)$ and m, reflecting the deviation of regional abatement efforts from the market equilibrium. The equation (2) simplifies to $\text{SCC}_i = \text{MAC}_i(E_i) - m$, where SCC_i denotes the regional SCC. A positive regional SCC implies $\text{MAC}_i(E_i) > m$, suggesting that a region experiencing climate damages has an incentive to abate emissions to a level where the marginal abatement cost exceeds the market price of emission permits.

In the environmental economics literature, it is well established that when production generates emissions as a negative externality in an economy, a regulator can achieve the socially efficient level of abatement by setting an emission cap at that level and issuing tradable permits to firms. The resulting market equilibrium under cap-and-trade is equivalent to the

[7] This assumption ensures that no region can abate more than its gross emissions solely to sell permits to other regions.

outcome of an optimal emission tax equal to the MAC at the efficient abatement level, in the absence of cost uncertainty or transaction costs. However, in a multi-region framework where climate damages are region-specific, the decentralized equilibrium outcome under the global ETS does not necessarily coincide with the regional social planner's optimal outcome. The underlying reason is that, because climate damages are heterogeneous across regions, a uniform global carbon price alone may not yield regionally optimal levels of emission abatement or the corresponding emission prices.

The intuition behind $\text{SCC}_i = \text{MAC}_i(E_i) - m$ can be further illustrated through an extreme case. If emission caps are sufficiently large such that they are not binding for any region—effectively a scenario without emission constraints—permit prices and trading volumes would be zero. Imposing the equilibrium condition $\text{MAC} = m$ in this situation would imply no abatement (i.e., $\text{MAC} = 0$ when $m = 0$). However, it is well established that even in the absence of binding caps, the optimal level of emission abatement from the perspective of a regional social planner remains strictly positive (i.e., $\text{SCC} = \text{MAC} > 0 = m$) under noncooperative Nash equilibrium (see, e.g., Nordhaus and Yang, 1996; Cai et al., 2023). This example further highlights the gap between the regional social planner's optimal abatement level and the decentralized market outcome, as firms undertake no abatement in the absence of an emission price. The basic intuition explored here carries over to the dynamic general equilibrium model introduced in the next section, where we further confirm numerically that $\text{SCC}_i = \text{MAC}_i(E_i) - m$ continues to hold.

An additional important implication of this relationship is that the two pricing instruments—emission taxes and cap-and-trade—are not competing policies but rather complementary under the global ETS framework. Although our model does not explicitly introduce firms, the regional MAC is effectively obtained as an aggregation of individual firms' marginal abatement quantities at a given price level within a region (Keohane and Olmstead, 2016). To achieve the optimal level of net emissions, E_i, *from each regional social planners perspective* under the global ETS, the optimal policy for each regional planner is to impose, within its own economy, a carbon tax equal to its regional SCC_i on top of the permit price from the global ETS. This ensures that individual firms internalize both the regional SCC and the global permit price. With the regional tax incorporated, each individual firm chooses net emissions such that its own MAC equals the sum of the permit price and the regional carbon tax, i.e., $\text{MAC}_\text{i}(E_i') = \tau_i + m'$, where the optimal carbon tax is $\tau_i = \text{SCC}_i$ from the perspective of the regional social planner.

For a partial ETS, if region i participates in the ETS, then the relation $\text{SCC}_i = \text{MAC}_i(E_i) - m$ still holds, where m is the equilibrium permit price between the participating regions; if region i does not participate, then the relation is changed to $\text{SCC}_i = \text{MAC}_i(E_i)$, which is a

standard relation under no ETS.

4 A Dynamic Regional Model of Climate and the Economy with an ETS

We now introduce a dynamic regional model of climate and economy that integrates a global ETS across multiple regions. Our model framework extends the RICE model (Nordhaus and Yang, 1996; Nordhaus, 2010b) by incorporating the global ETS in a dynamic setting and the TCRE climate system with annual time steps. One of the main focuses of the model is to characterize the equilibrium path of carbon prices in a noncooperative environment, where a social planner of each region maximizes its own social welfare by optimally choosing emissions abatement, permit purchases in the global carbon market, and consumption over time. Future regional emissions are constrained by emission caps based on commitments established under the Paris Agreement, later updated by the Glasgow Pact, and by net-zero targets.

The macroeconomic framework of our model employs a multi-regional representation of the Ramsey growth model. Each region is indexed by $i \in \mathcal{I}$, where $\mathcal{I}$ is the set of regions. Time is discrete and infinite, with annual time steps indexed by $t = 0, 1, 2, \cdots$. All agents are forward-looking with complete information. The model presented here abstracts from uncertainty, excludes international trade of goods other than emission permits, and assumes frictionless trading in the ETS.

4.1 The Economic System

Each region consists of a representative household with a population size of $L_{i,t}$, and utility of the representative consumer is given by

$$u(c_{i,t}) = \frac{c_{i,t}^{1-\gamma}}{1-\gamma}, \tag{3}$$

where $c_{i,t}$ is per capita consumption and γ is the inverse of intertemporal elasticity of substitution. Following DICE-2016R (Nordhaus, 2017), γ is set to 1.45.

There is a representative firm in each region that employs a Cobb-Douglas production technology using capital and labor as inputs, and produces a numeraire good whose price is normalized to 1. The representative household owns all input factors and the firm of the regional economy. The gross output, or pre-damage output, $Q_{i,t}$, is given by

$$Q_{i,t} = A_{i,t} K_{i,t}^{\alpha} L_{i,t}^{1-\alpha}, \tag{4}$$

where $K_{i,t}$ is capital stock, and $\alpha = 0.3$ is the elasticity of gross output with respect to capital, as in Nordhaus (2017). Consistent with the standard neoclassical growth model, capital depreciates over time, and the firm invests to replenish and accumulate capital stock. The evolution of capital follows

$$K_{i,t+1} = (1 - \delta) K_{i,t} + I_{i,t}, \tag{5}$$

where $I_{i,t}$ is investment and $\delta = 0.1$ is the rate of depreciation of capital stock.

Regions experience climate damages resulting from the externalities of global emissions, with the extent of these damages varying across regions. The output net of climate-induced damages, denoted as $Y_{i,t}$, is given by:

$$Y_{i,t} = \left(\frac{1}{1 + \pi_{1,i} T_t + \pi_{2,i} T_t^2} \right) Q_{i,t}, \tag{6}$$

where $\pi_{1,i}$ and $\pi_{2,i}$ are region-specific climate damage parameters, and T_t is the global average temperature increase in degrees Celsius above the pre-industrial level. The specification captures the adverse (or potentially beneficial for some regions) effects of rising global average temperature, where local damages increase nonlinearly with temperature, following the quadratic form commonly used in the climate economics literature (Nordhaus, 2014, 2017).

4.2 Emissions

Each region's economic activity produces carbon emissions, and the representative firm faces emission constraints of the region. The *gross emissions* before abatement, in gigatonnes of carbon (GtC), is assumed to be proportional to the gross output for region i at time t:

$$E_i^{\text{Gross}} = \sigma_{i,t} Q_{i,t}, \tag{7}$$

where $Q_{i,t}$ is the gross output, and $\sigma_{i,t} > 0$ is the exogenous carbon intensity. The firm may choose to reduce a fraction of gross emissions, with its efforts represented by emission control rate $\mu_{i,t} \in [0, 1]$.[8] The *amount of emissions abated* by each region, $E_{i,t}^A$, is then expressed as

[8] Alternatively, abatement can also be modeled through the reduced use of fossil fuel energy inputs in the production function (see, e.g., Bosetti et al., 2006; Bauer et al., 2012; Golosov et al., 2014; Baldwin et al., 2020). However, such models often require disaggregation of fossil fuel energy firms, renewable energy firms, final-goods producers, and other sectors, increasing the complexity of the model. The emission control rate approach simplifies this by offering a more streamlined representation.

follows.

$$E^A_{i,t} = \mu_{i,t}\sigma_{i,t}Q_{i,t}. \tag{8}$$

The emission abatement efforts incur costs to the firm and are heterogeneous across regions due to technological differences. The emission abatement cost, $\Phi_{i,t}$, is specified as

$$\Phi_{i,t} = b_{1,i,t}\mu^{b_{2,i}}_{i,t}Q_{i,t}, \tag{9}$$

where $b_{1,i,t} = (b_{1,i} + b_{3,i}\exp(-b_{4,i}t))\sigma_{i,t}$. The parameters $b_{1,i}$, $b_{2,i}$, $b_{3,i}$, and $b_{4,i}$ govern the cost structure of emission abatement cost, $\Phi_{i,t}$, which depends on both the gross output $Q_{i,t}$ and the exponential function of the emission control rate, $\mu_{i,t}$. This specification captures the dynamic nature of abatement costs, reflecting potential technological advancements that reduce the cost of emissions abatement over time.

In a global ETS, or a cap-and-trade system, each region is provided with an emission allowance and can trade emission permits with other regions. The representative firm in each region that emits beyond its cap can purchase permits, while those emitting below their allowance can sell excess permits. Denoting the *emissions net of abatement* (*net emissions*) as $E_{i,t} = E^{\text{Gross}}_i - E^A_{i,t}$, the emission cap constraint is represented by

$$E_{i,t} - E^P_{i,t} \leq \overline{E}_{i,t}, \tag{10}$$

where $\overline{E}_{i,t}$ is the *emission cap* assigned to region i at time t, and $E^P_{i,t}$ denotes the amount of *emissions purchased* from other regions. Note that $E^P_{i,t} > 0$ indicates that region i is a net buyer of emission permits at time t, while $E^P_{i,t} < 0$ implies region i is a net seller of emission permits at time t. In a model that does not consider emission permit trade, the emissions purchase is simply set at $E^P_{i,t} = 0$ for all i and t.

4.3 The Climate System

The global average temperature rises as carbon emissions accumulate in the atmosphere. Adopting the TCRE climate system representation (Matthews et al., 2009), it is assumed that the global average temperature increase above the pre-industrial level is approximately linear to cumulative global emissions $\mathcal{E}_t$, i.e.,

$$T_t = \zeta\mathcal{E}_t, \tag{11}$$

where ζ represents the contribution rate of cumulative global emissions to temperature. The cumulative global emissions evolve according to

$$\mathcal{E}_{t+1} = \mathcal{E}_t + \sum_{i \in \mathcal{I}} E_{i,t}. \tag{12}$$

This dynamic process captures the accumulation of emissions in the atmosphere over time, with each region contributing to the global emissions stock and, consequently to the increase in global temperature.

4.4 Market Clearing

The goods market clearing implies that the total consumption of each region under the ETS is constrained by

$$c_{i,t} L_{i,t} = Y_{i,t} - I_{i,t} - \Phi_{i,t} - m_t E^P_{i,t}, \tag{13}$$

where m_t is the market equilibrium price of emission permits. As in the static framework, the last term on the right-hand side reflects the cost or revenue generated from the emission permit trade.

Finally, the emission trading market clears each period, given by:[9]

$$\sum_{i \in \mathcal{I}} E^P_{i,t} = 0. \tag{14}$$

If it is a partial ETS and region i does not participate in the partial ETS, then we set $E^P_{i,t}$ to be fixed at zero.

5 Solving for the Equilibrium

Building on the model components outlined in Section 4, we now define the noncooperative equilibrium of our multi-region dynamic model with the ETS and present an algorithm used to obtain the Nash Equilibrium solution.

[9]The current model assumes that intertemporal lending or borrowing of emission permits is not allowed.

5.1 The Noncooperative Equilibrium

In the noncooperative model, the regional social planner of each region maximizes the region's own lifetime social welfare. The maximization problem for each region i is defined as

$$\max_{c_{i,t},E^P_{i,t},\mu_{i,t}} \sum_{t=0}^{\infty} \beta^t u(c_{i,t}) L_{i,t}, \tag{15}$$

where β is the discount factor. We follow DICE-2016R (Nordhaus, 2017) and set $\beta = 0.985$. Since one region's emissions will influence the global average temperature, and therefore other regions' output, the maximization problems of all regions have to be solved simultaneously as a dynamic game. Then we define the dynamic Nash equilibrium of the economy as follows.

DEFINITION: Given the initial capital and cumulative global emissions, $\{K_{i,0}, \mathcal{E}_0 : \ i \in \mathcal{I}\}$, and the exogenous paths of emission caps $\{\overline{E}_{i,t} : \ i \in \mathcal{I}, t \geq 0\}$, the dynamic Nash equilibrium for the noncooperative model is a sequence of quantities $\{c_{i,t}, E^P_{i,t}, \mu_{i,t}, K_{i,t}, \mathcal{E}_t, T_t : i \in \mathcal{I}, t \geq 0\}$ and prices $\{m_t : \ t \geq 0\}$ that simultaneously solve the maximization problem (15) for all regions subject to equations (3)-(14).

The optimal solution for this dynamic multi-region model involves three choice problems. First, as in the standard Ramsey-type growth model, each region faces an intertemporal choice problem in which there is a trade-off between current consumption and future consumption. Each region may sacrifice present consumption to make investments, which can contribute to higher consumption in the future. Second, the intertemporal choice problem is further compounded by climate damages. Current production increases the global temperature, which subsequently lowers future productivity. Since emissions abatement has positive externalities, a region's returns from abatement efforts may not be large enough to offset the cost of abatement. Therefore, the optimal solution of each region is highly dependent on the choices made by other regions. Lastly, the ETS allows each region to choose between purchasing emission permits from the market and undertaking further abatement. The ETS promotes efficient abatement globally by encouraging regions with better abatement technology or capacity (thus, with lower abatement cost) to conduct more abatement, and regions with less efficient abatement technology to purchase permits from other regions.

Note that the equilibrium concept in our noncooperative model is an Open-Loop Nash equilibrium (OLNE), which provides a solution path over time depending on the initial state. In an OLNE, regions commit to the strategies over time for their decision variables—consumption ($c_{i,t}$), emission purchase ($E^P_{i,t}$), and emission control rate ($\mu_{i,t}$)— at the initial period and cannot change their behavior over time. This concept contrasts with the Markov Perfect Equilibrium (MPE), where regions may make multiple decisions over time, allowing

adaptation in their strategies. While the OLNE concept may be less satisfactory than the MPE concept (since OLNE is not subgame perfect), it has the computational advantages of solving open-loop versus feedback, particularly when the dimension of the state space is large and there are occasionally binding constraints as in our case.

5.2 The Algorithm for the Noncooperative Model

Obtaining the optimal solution of the dynamic model involving multiple regions under non-cooperation is challenging. In particular, finding an equilibrium solution for the emission permit prices that satisfies the optimality conditions for each region as well as the market clearing condition poses significant computational challenges.

Here we outline the algorithm we develop to obtain the optimal solution for our model. With the discount factor $\beta = 0.985$, the discounted utilities after 300 years are nearly zero and have little impact on the solution in the first 100 years. Let

$$V_{i,300}(K_{1,300}, ..., K_{12,300}, \mathcal{E}_{300}) = u\left(\frac{0.75Y_{i,300}}{L_{i,300}}\right)\frac{L_{i,300}}{1-\beta}$$

be a terminal value function at the terminal year 300, which approximates the present value of utilities after 300 years, assuming that consumption at any $t \geq 300$ is equal to 75 percent of the output $Y_{i,300}$ at $t = 300$ and that the exogenous population after 300 years stays at its value at $t = 300$. Note that $Y_{i,300}$ is computed with a function of the terminal state $K_{i,300}$ and $\mathcal{E}_{300}$. Thus, we can transform the infinite horizon models to finite horizon models, where region i's social welfare is rewritten as

$$\sum_{t=0}^{299} \beta^t u(c_{i,t})L_{i,t} + \beta^{300} V_{i,300}(K_{1,300}, ..., K_{12,300}, \mathcal{E}_{300}),$$

We also numerically verify that this time horizon truncation at 300 years has little impact on the OLNE solution in the first 100 years, by solving the same model but with a time horizon truncation at 400 years. This time horizon truncation method is common in solving infinite-horizon non-stationary models. For example, DICE-2016 truncates its model's infinite horizon to 500 years, with a terminal value function being zero everywhere, for obtaining its numerical solution.

The algorithm to solve the noncooperative model is as follows:

Step 1. *Initialization.* Set an initial guess of permit prices $\{m_t^0 : \ t \geq 0\}$, and emissions $\{E_{i,t}^0 : \ t \geq 0\}$. Iterate through steps 2, 3 and 4 for $j = 1, 2, ...,$ until convergence.

Step 2. *Maximization Step* at iteration j. For each region i, solve the maximization problem (15) without the market clearing condition (14), assuming the permit prices $\{m_t^{j-1} : t \geq 0\}$ and other regions' emissions $\{E_{i',t}^{j-1} : \ i' \neq i, \ t \geq 0\}$ are given from the initialization step when $j = 1$ or Step 3 at iteration $j-1$ when $j > 1$. The optimal emissions and permits purchased for region i are denoted $\{E_{i,t}^{*,j}, E_{i,t}^{P,j} : \ t \geq 0\}$.

Step 3. *Update Step* at iteration j. After solving for the optimization problem of all regions respectively in Step 2, update the permit prices and emissions as

$$\begin{aligned} m_t^j &= m_t^{j-1} \exp\left(\omega \sum_{i \in \mathcal{I}} E_{i,t}^{P,j}\right), \\ E_{i,t}^j &= \omega E_{i,t}^{*,j} + (1-\omega) E_{i,t}^{j-1}, \quad \forall i \in \mathcal{I}, \end{aligned}$$

where $\omega = 0.1$ is a weight parameter and $\sum_{i \in \mathcal{I}} E_{i,t}^{P,j}$ is the net quantity of traded emission permits.

Step 4. *Check the convergence criterion.* Check if $m_t^j \simeq m_t^{j-1}$, $E_{i,t}^j \simeq E_{i,t}^{j-1}$, and $E_{i,t}^{P,j} \simeq E_{i,t}^{P,j-1}$ for every region i and $t \geq 0$. If so, stop the iteration, otherwise go to Step 2 by increasing j with 1. Note that $m_t^j = m_t^{j-1}$ implies that the market clearing condition (14) holds at the solution.

This algorithm embodies the concept of market equilibrium. When there is a net positive quantity of traded emission permits in the market, indicating excess demand, we increase the permit prices. Conversely, when there is a net negative quantity of traded emission permits, indicating excess supply, we lower the permit prices. This mechanism ensures that the market reaches a balance between supply and demand, and thus the market clears. Furthermore, this algorithm guarantees that each region obtains its optimal solution and reaches an equilibrium state. In other words, no region has the incentive to deviate from the Nash equilibrium for the noncooperative model solution.

6 Data and Calibration

When taking our model to data, two key objectives are pursued. The first objective is to generate regional emission cap pathways ($\overline{E}_{i,t}$) for future periods, constraining the constituent nations of each region to meet their emissions commitments under the Glasgow Pact and the long-term net zero emission targets. The second objective is to determine parameters for total factor productivity ($A_{i,t}$), carbon intensity ($\sigma_{i,t}$), abatement cost ($b_{1,i}$, $b_{2,i}$, $b_{3,i}$, $b_{4,i}$), and climate damage ($\pi_{1,i}, \pi_{2,i}$) that reflect the future projections provided in recent studies

(Burke et al., 2018; Ueckerdt et al., 2019; Kahn et al., 2021). We obtain these region-specific parameters, which capture regional heterogeneities in GDP growth, emissions, technologies, and climate damages.

We assume that the world is divided into 12 aggregated regions: the United States (US), the EU, Japan, Russia, Eurasia, China, India, Middle East (MidEast), Africa, Latin America (LatAm), Other High-Income countries (OHI) and other non-OECD Asia (OthAs). These 12 regions are formed by aggregating 152 countries around the world, following the regional classification in the RICE model (Nordhaus and Yang, 1996; Nordhaus, 2010b).[10] Note that, while we present our simulation results at a regionally aggregated level for computational tractability, our methods are applicable to a larger number of regions and can be readily extended to obtain country-level outcomes. For example, the regional SCC for Africa can be disaggregated to approximate country-level SCCs, since the regional SCC is equal to the sum of the SCCs of the individual countries within the region. [11] The initial year is set to 2020, with country-level historical data on population (billions), capital ($ trillions, 2020), GDP ($ trillions, 2020), and emissions (CO_2 equivalent, GtC) sourced from the World Bank. [12] For future population pathways, projections from the SSP2 scenario (Samir and Lutz, 2017) are employed.

6.1 Regional Emission Cap Pathways

Since there is no global cap-and-trade system or ETS currently in place, we consider the emission commitments outlined in the Paris Agreement and the COP26 Glasgow Climate Pact. Under the Paris Agreement, 195 countries or regions set Nationally Determined Contributions (NDCs) that specify their near-term targets for 2025 or 2030, along with long-term net-zero commitments for 2050 to 2070. These near-term targets were further strengthened during the Glasgow Climate Pact in 2021, with most countries and regions submitting updated or new NDCs.[13] We collect reports of the most updated NDCs after the Glasgow Climate Pact and obtain the target years to reach net zero emissions of different countries from Climate Action Tracker.[14] Based on these datasets, we create the baseline regional emission cap pathways for future periods following the strategy detailed below.

[10] See Appendix 1 A.2 for the full list of countries and regional aggregation.

[11] Regional SCC is the present value of future climate damages in a region resulting from an additional unit of global emissions released in the current period.

[12] To obtain initial capital stock, we used capital formation data from the World Bank. Specifically, we computed $K_{i,2020} = \sum_{g=0}^{20}(0.9)^g \mathrm{CF}_{i.2020-g}$, where $\mathrm{CF}_{i,t}$denotes capital formation adjusted to 2020 values in trillions of USD.

[13] Individual NDC documents were obtained from the following source: UNFCCC NDC Registry (https://unfccc.int/NDCREG)

[14] See https://climateactiontracker.org/.

As the first step, we obtain the near-term emission targets for each country. In their NDC reports, most countries express targets as a specific percentage reduction in emissions by 2030 (or, in some cases, 2025) compared to their Business As Usual (BAU) emission level at some base year. Some countries, including China, Chile, Malaysia, Singapore, and Tunisia specified their targets as a percentage reduction in carbon intensity instead of a percentage reduction in emissions. For the countries that did not make a specific emissions reduction pledge, we assume that their carbon intensity reduction and emission reduction percentages are the same as those of the most populous country in that region.

Next, we generate annual emission cap pathways based on the regions' historical emission levels (World Bank, 2020), their emission targets for 2030 (or 2025), and net zero emission target years. We use five-year emissions data (2014 - 2018) from the World Bank and the INDC emission targets in 2030 (or 2025) to fit a quadratic function and use this fitted function to project the emission pathways for the periods between 2018 and 2030. Emission projections for the years between 2030 (or 2025) and the net zero emission target year are obtained by linearly interpolating the emissions. After obtaining the country-level emission pathways, we aggregate them to find the regional emission cap pathways.[15] To assess the implications of varying stringency in the emission caps, we also create additional emission cap pathways by choosing alternative net zero scenarios, wherein we assume that all regions achieve net zero emissions by 2050 (most stringent), 2070, or 2090 (most lax). See Figures A.5 and A.6 in Appendix A.3.4 for the regional emission cap pathways in the baseline cap scenario and the different emission cap pathways at the global level.

6.2 Total Factor Productivity and Climate Damage

We follow Cai et al. (2023) to calibrate total factor productivity (TFP), $A_{i,t}$, and the climate damage parameters $\pi_{1,i}$ and $\pi_{2,i}$, based on Burke et al. (2018), who provide the projected GDP of 165 countries till 2099 assuming no climate-related impacts, and their GDP assuming the contemporaneous climate impact of the RCP4.5 temperature $T_t^{\text{RCP4.5}}$[16] until 2049, under the SSP2 population pathway.[17] We aggregate these projections according to our 12 regions and employ the SSP2 population scenario to obtain regional GDP per capita estimates, $y_{i,t}^{\text{BDD,NoCC}}$ under no climate impact and $y_{i,t}^{\text{BDD}}$ under climate impact, which are used to

[15] We also find that our aggregated regional emission cap pathways are close to those used in Nordhaus (2010b).

[16] We choose the RCP4.5 scenario instead of the other RCP scenarios, because the RCP4.5 scenario is the closest which covers the range of temperature in our solution.

[17] It is nontrivial to use historical data to calibrate future TFP, particularly when we need to isolate the climate impacts from the data. For simplicity, we use the projected GDP for the calibration in this paper. We also use the TFP growth values in RICE to do sensitivity analysis, and find our results are still robust (see Appendix A.4.7).

calibrate the regional TFP, $A_{i,t}$, and the climate damage parameters, $\pi_{1,i}$ and $\pi_{2,i}$. For each region i, the dynamic path of the TFP is modeled by the relationship $A_{i,t+1} = A_{i,t} \exp(g_{i,t})$, where $g_{i,t}$ is the growth rate of $A_{i,t}$ at time t. When $t < 80$ (i.e., within this century), we assume

$$g_{i,t} = g_{i,0} \exp(-d_i t). \tag{16}$$

For $t \geq 80$ (i.e., beyond this century), since the cumulative effect is huge for a long horizon, it is often inappropriate to simply extrapolate TFP growth rate using the formula (16). Therefore, we follow RICE to generate $g_{t,i}$ for $t \geq 80$. See Appendix A.3.5 for the details.

In our structural estimation, we obtain $(g_{i,0}, d_i, \pi_{1,i}, \pi_{2,i})$ by solving the following minimization problem:

$$\min_{g_{i,0}, d_i, \pi_{1,i}, \pi_{2,i}} \sum_{t=0}^{79} \left(\frac{y_{i,t}^{\text{NoCC}}}{y_{i,0}^{\text{NoCC}}} - \frac{y_{i,t}^{\text{BDD,NoCC}}}{y_{i,0}^{\text{BDD,NoCC}}} \right)^2 + \sum_{t=0}^{29} \left(\frac{y_{i,t}}{y_{i,0}} - \frac{y_{i,t}^{\text{BDD}}}{y_{i,0}^{\text{BDD}}} \right)^2. \tag{17}$$

Here $y_{i,t}^{\text{NoCC}}$ is GDP per capita obtained under no climate impact by solving the following optimal growth model with a choice of $(g_{i,0}, d_i, \pi_{1,i}, \pi_{2,i})$ and its associated TFP A_{it}:

$$\begin{aligned} \max_{c_{i,t}} \quad & \sum_{t=0}^{\infty} \beta^t u(c_{i,t}) L_{i,t}, \\ \text{s.t.} \quad & K_{i,t+1} = (1-\delta) K_{i,t} + \left(y_{i,t}^{\text{NoCC}} - c_{i,t} \right) L_{i,t}, \end{aligned} \tag{18}$$

where $y_{i,t}^{\text{NoCC}} = A_{i,t} K_{i,t}^{\alpha} L_{i,t}^{-\alpha}$ and $u(c_{i,t})$ is defined as in equation (3); and $y_{i,t}$ is GDP per capita under climate impact by solving the following optimal growth model:

$$\begin{aligned} \max_{c_{i,t}} \quad & \sum_{t=0}^{\infty} \beta^t u(c_{i,t}) L_{i,t}, \\ \text{s.t.} \quad & K_{i,t+1} = (1-\delta) K_{i,t} + (y_{i,t} - c_{i,t}) L_{i,t}, \end{aligned} \tag{19}$$

where

$$y_{i,t} = \frac{1}{1 + \pi_{1,i} T_t^{\text{RCP4.5}} + \pi_{2,i} \left(T_t^{\text{RCP4.5}} \right)^2} A_{i,t} K_{i,t}^{\alpha} L_{i,t}^{-\alpha}.$$

The initial TFP $A_{i,0}$ is chosen such that $A_{i,0} K_{i,0}^{\alpha} L_{i,0}^{-\alpha} / (1 + \pi_{1,i} T_0 + \pi_{2,i} T_0^2)$ is equal to the observed GDP per capita in 2020. Figures A.2 and A.3 in Appendix A.3.2 shows that with our calibrated $(g_{i,0}, d_i, \pi_{1,i}, \pi_{2,i})$, the GDP per capita $y_{i,t}^{\text{NoCC}}$ or $y_{i,t}$ matches well with the projected data $y_{i,t}^{\text{BDD,NoCC}}$ or $y_{i,t}^{\text{BDD}}$ from Burke et al. (2018), respectively, for all regions.

6.3 Carbon Intensity

To obtain the time-varying and region-specific carbon intensities $\sigma_{i,t}$, we use the projections of GDP and emissions in Ueckerdt et al. (2019), who report simulation results of future emissions and GDP under different scenarios based on climate policy regimes, technology portfolios, and carbon tax implementation. As the carbon intensity in our model reflects the zero-carbon tax regime, we employ results from the scenario defined as 'FFrun111' in Ueckerdt et al. (2019). Specifically, this FFrun111 scenario corresponds to climate action from 2010 with full technology portfolio and no carbon tax. . Based on the equation (7), we calculate the carbon intensities as $\sigma_{i,t} = E^U_{i,t,\text{FFrun111}}/Q_{i,t,\text{FFrun111}}$, where $E^U_{i,t,\text{FFrun111}}$ and $Q_{i,t,\text{FFrun111}}$ are the projected regional emissions and GDP under the FFrun111 scenario for region i at time t. [18]

6.4 Abatement Cost

Our estimation of the abatement cost parameters $b_{1,i}$, $b_{2,i}$, $b_{3,i}$, and $b_{4,i}$ relies on the simulation results under ten different levels of carbon taxes in Ueckerdt et al. (2019). For each scenario j with associated carbon taxes $\tau^U_{t,j}$ for every region i, Ueckerdt et al. (2019) report the projected regional emissions net of abatement ($E^U_{i,t,j}$), for region i at time t. Since Ueckerdt et al. (2019) do not consider an ETS, according to the discussion in Section 3, we can assume that their carbon taxes $\tau^U_{t,j}$ are equal to the marginal abatement costs when emissions are strictly positive. That is,

$$\tau^U_{t,j} = \frac{1,000 b_{2,i} \mu_{i,t,j}^{b_{2,i}-1} b_{1,i,t}}{\sigma_{i,t}} = 1,000 b_{2,i} \mu_{i,t,j}^{b_{2,i}-1} (b_{1,i} + b_{3,i} \exp(-b_{4,i} t)), \tag{20}$$

for $\mu_{i,t,j} \in (0,1)$. Therefore, we can use their simulation results under different carbon tax levels to estimate $b_{1,i}$, $b_{2,i}$, $b_{3,i}$, and $b_{4,i}$. At first, we estimate the associated emission control rate $\mu^U_{i,t,j}$ using the equations (7)-(8) as follows:

$$\mu^U_{i,t,j} = 1 - \frac{E^U_{i,t,j}}{E^U_{i,t,\text{FFrun111}}}, \tag{21}$$

where $E^U_{i,t,\text{FFrun111}}$ is the regional emission from the FFrun111 scenario with zero carbon tax (see Ueckerdt et al. (2019) for details). Then we use the computed $\mu^U_{i,t,j}$ and the associated

[18] Ueckerdt et al. (2019) provide data for 11 regions. Upon comparison, we find that the countries constituting the 'Rest of the World (ROW)' region are the ones that are in the 'Other High Income (OHI)' and 'Eurasia' region in our study. Therefore, the carbon intensity obtained from the ROW in Ueckerdt et al. (2019) corresponds to that of OHI and Eurasia regions in our work.

carbon tax $\tau^U_{t,j}$ to find the abatement cost coefficients—$b_{1,i}$, $b_{2,i}$, $b_{3,i}$, and $b_{4,i}$—such that the equality (20) can hold in an approximate manner for every scenario j and time t.

6.5 Climate System: Transient Climate Response to Emissions

In the TCRE climate system, $\mathcal{E}_0$, is chosen such that the initial global mean temperature T_0 in year 2020 is 1.2 degrees Celsius above the pre-industrial level. The contribution rate of cumulative global emissions to temperature is calibrated at $\zeta = 0.0021$ by using the projections of emissions and temperatures across the four Representative Carbon Concentration Pathways (RCPs) scenarios: RCP 2.6, RCP 4.5, RCP 6.0, and RCP 8.5 (Meinshausen et al., 2011). That is, we solve the following minimization problem:

$$\begin{aligned} \min_{\zeta} \quad & \sum_t \sum_j \left\| T^j_t - \zeta \mathcal{E}^j_t \right\| \\ s.t. \quad & \mathcal{E}^j_{t+1} = \mathcal{E}^j_t + E^j_t, \ \forall t, j, \end{aligned}$$

where j represents one of four RCP scenarios, E^j_t and T^j_t are the exogenous projections of emissions and temperatures, respectively, at time t for RCP scenario j. Figure A.1 in Appendix A.3.1 demonstrates that the calibrated TCRE climate system matches well all four RCP temperature pathways using their associated RCP emission pathways.

7 Baseline Model Results

This section presents the numerical simulation results under the assumption that all regions participate in the global ETS. The baseline emission cap scenario is defined in accordance with the NDCs in the near term and the net-zero targets in the mid- to long term. We report the results through the end of the century (2020–2100), focusing on both economic and environmental outcomes across key variables. Additionally, we provide an in-depth analysis of the numerical simulation results to evaluate the effects of implementing a global cap-and-trade system.

7.1 Emissions, Temperature, and Permit Prices

Figure 1 displays key simulation results at the global level, from the noncooperative model with the ETS under the baseline emission cap scenario. Until 2100, we can delineate three periods according to the global emission trading patterns. Prior to 2024, global emissions do not reach the global emission caps and therefore the permit price remains zero, implying

an excess supply of emission permits in the initial years (Figure 1 top-left and bottom-left), as the emission caps in the initial years are large while they become much smaller over time (Figure A.5). This result is not surprising, considering that an oversupply of emission permits has been observed in the EU ETS (Fuss et al., 2018), resulting in zero or very low permit prices. During this period, the volume of global emission abatement and its associated abatement cost remain at low levels (Figure 1 top-left and bottom-right). This result implies that the global emission cap should be set at a level such that there is no over-supply of emission permits, so that permit prices are strictly positive under noncooperation and the ETS.

Global emissions are constrained by the global emission caps starting from 2024. To comply with the monotonically decreasing emission caps, the regions undertake additional abatement efforts and/or purchase emission permits. This results in a substantial increase in the volume of emission abatement, along with the abatement cost and permit price. The decrease in global emissions is mainly achieved by the concomitant increase in global abatement, which peaks by around 2070 (Figure 1 top-left). The global abatement cost also increases steeply to reach its maximum value of \$7.82 trillion by 2070, and then decreases as the world reaches net zero emissions by 2070. The emission permit trade also gradually decreases to zero by 2070 (Figure 1 top-left). As the emission cap becomes tighter over the years, the permit price increases to \$923 per ton of carbon in 2050 and \$2,105 in 2069 (Figure 1 bottom-left). The kinks in the permit price path in 2030 result from a kink in emission cap pathways (see Figure A.6), while those in 2050 and 2060 are a result of some regions achieving net zero emissions, as shown in Figure A.5. Essentially, binding emission caps lead to a rise in the overall emission abatement, while the steep increase in the permit price limits the trading of emission permits.

Post-2070 is the period when global emissions are at net zero. For this period, emission permits are no longer traded and all emissions are abated in each region.[19] By the end of this century, the atmospheric temperature is projected to reach 1.7 degrees Celsius above the pre-industrial level, which is driven by net positive emissions before 2070 (Figure 1 top-right), restricted by the emission caps.[20] Lastly, the global climate damage rises almost linearly over the entire period (Figure 1 bottom-right). Overall, our noncooperative model simulation predicts that the global emission caps set by the Paris Agreement and Glasgow Pact are not restrictive enough to achieve the global target of limiting the temperature rise to 1.5 degrees Celsius.

[19] In the bottom-left panel of Figure 1, we plot the emission permit price only when the traded volume is positive.

[20] If there is no emission cap, then the temperature anomaly will be much higher. This can be seen in a later discussion with alternative emission caps.

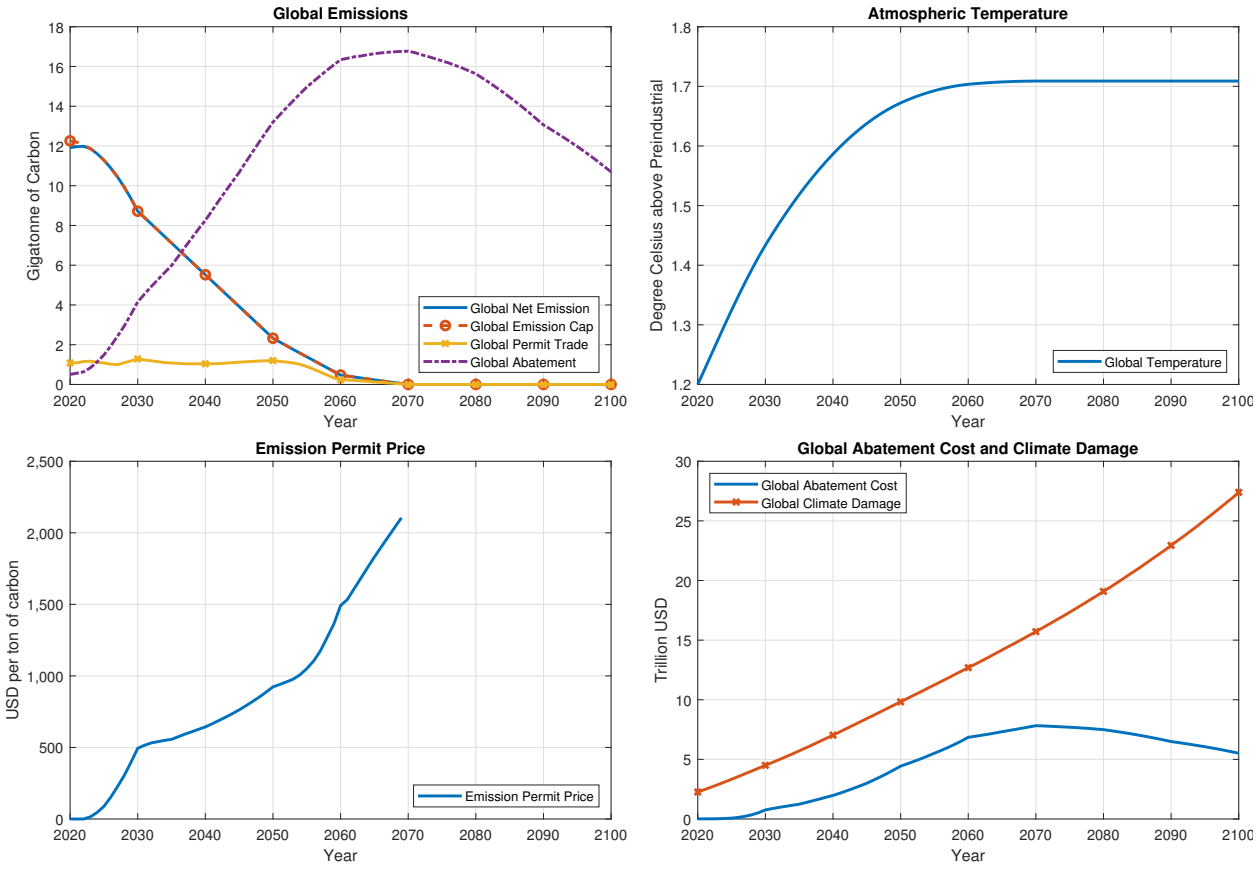

Figure 1: Simulation results at the global scale under the baseline emission cap scenario.

It is instructive to examine the trading patterns of different regions in the emission permit market over the years to identify the permit buyers and sellers. Figure 2 displays the volumes of traded emission permits for each region over time, with a positive value denoting permit purchase and a negative value indicating permit sales. Before 2024, although there is an excess permit supply at the global level, the emission cap constraint is effective for some regions, such as China and Latin America, as these regions become permit buyers at this early stage. After 2024, when the global emission cap constraint becomes binding, the group of permit buyers consists of the US, EU, India, and OHI regions; the group of permit sellers consists of Russia, China, and Eurasia, with China being the largest permit provider after 2032. Japan is expected to be involved in a relatively small volume of permit trading, and the other regions (Africa, MidEast, Latin America, and OthAs) change their status of permit suppliers to buyers or vice versa over time.

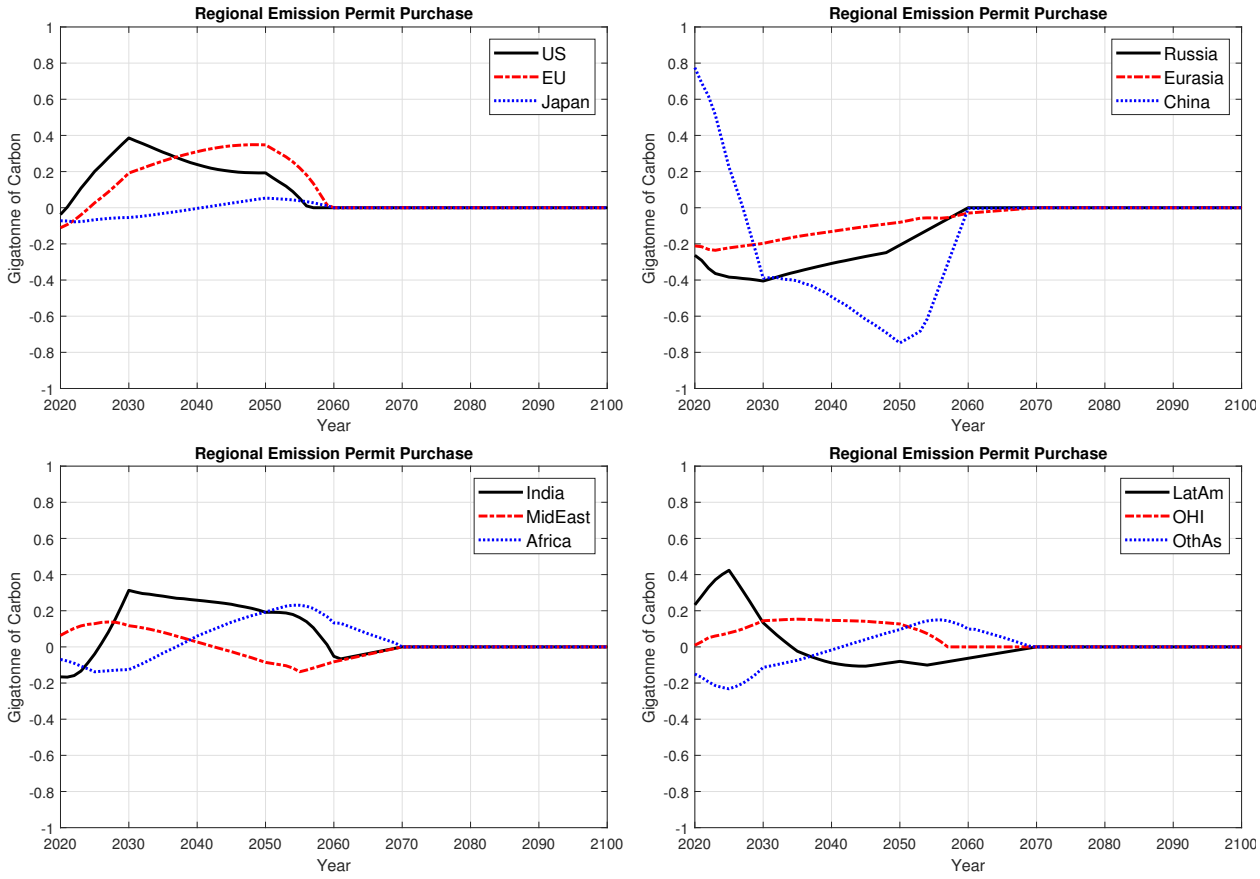

Figure 2: Simulation results of regional emission permit purchase under the baseline emission cap scenario.

7.2 Regional MAC and SCC

Based on the simulation results under the baseline emission cap scenario, this section examines the relationship between the regional MAC, SCC, and the market equilibrium emissions permit price under the global ETS regime. The MAC captures the additional cost incurred due to an increase in emission abatement. From our model equation (8), the total abatement cost is $\Phi_{i,t} = b_{1,i,t}\mu_{i,t}^{b_{2,i}}Q_{i,t}$, in trillions of USD. Thus, the MAC, in 2020 USD per ton of carbon, is obtained as follows:

$$\text{MAC}_{i,t} = 1,000\left(\frac{\partial\Phi_{i,t}}{\partial E_{i,t}^{A}}\right) = 1,000\left(\frac{b_{1,i,t}b_{2,i}\mu_{i,t}^{b_{2,i}-1}}{\sigma_{i,t}}\right). \tag{22}$$

Note that, with $b_{1,i,t} > 0$ and $b_{2,i} > 2$, MAC is strictly increasing on emission control rate $\mu_{i,t} \in [0,1]$.[21] Figure 3 displays the regional MAC along with the market equilibrium price of emission permits. The simulation result shows that, for most regions, the MAC increases

[21] See Table A.2 in Appendix A.1 for the list of our calibrated abatement cost parameters.

rapidly and remains strictly greater than the permit price until the emissions hit zero by 2050s or 2060s. [22] Russia is an exception, where the MAC falls below the permit price starting in 2021, which we will elaborate shortly in the next paragraph. The MAC of each region gradually decreases below the permit price after its net zero emission level is achieved (i.e., $E^*_{i,t} = 0$). Russia is the first region to achieve net zero emissions in 2048 (as shown in Figure A.7 in Appendix A.4.1). However, Russia continues to sell permits afterwards, as shown in Figure 2, because its net zero emission target year is 2060, under the baseline emission cap scenario. After 2048, Russia's MAC begins to decline slightly and stabilizes over time, as its emission control rate reaches its upper limit.[23] Similar trends are observed in other regions as they attain net zero emissions in the 2050s (China, Latin America, MidEast, the US, the OHI, Eurasia) and the 2060s (the EU, Japan and India). Africa and OthAs are the last group of regions to achieve net zero emissions (before trading of permits) by 2070, after which emission permits are no longer traded, and the MACs of all regions decline slowly over time. Note that if a region's after-permit-trade zero emission cap constraint is binding (i.e., the inequality (10) is binding with $\overline{E}_{i,t} = 0$), then even when its regional MAC is smaller than the permit price, the region will not be able to sell emission permits, otherwise it will violate the constraint.

The SCC, a central concept in the climate change literature, is widely used to quantify the present value of climate damages induced by an additional unit of carbon emissions. While the SCC is often calculated in a global social planner's problem (e.g., the DICE model), we consider the SCC for each region. Similar to van der Ploeg and de Zeeuw (2016) and Cai et al. (2023), we define the noncooperative SCC of a region as the marginal rate of substitution between global emissions and regional capital as follows:

$$\mathrm{SCC}_{i,t} = \frac{-1,000(\partial V_{i,t}/\partial \mathcal{E}_t)}{\partial V_{i,t}/\partial K_{i,t}}, \tag{23}$$

where $V_{i,t}$ is the value function of the noncooperative model at time t for region i, depending on the state variables $\{K_{i,t}, \mathcal{E}_t : \ i \in \mathcal{I}\}$; that is,

$$V_{i,t}(K_{1,t}, ..., K_{12,t}, \mathcal{E}_t) = \max_{c_{i,s}, E^P_{i,s}, \mu_{i,s}} \sum_{s=t}^{\infty} \beta^{s-t} u(c_{i,s}) L_{i,s},$$

for each region i under the open loop Nash equilibrium.[24] Since our cumulative global

[22] For regional optimal emissions, see Figure A.7 in Appendix A.4.1.

[23] When emission control rates are one, the MACs are $1,000 b_{2,i}(b_{1,i} + b_{3,i}\exp(-b_{4,i}t))$, and they are nearly constant when t is large.

[24] To compute the regional SCC in the noncooperative model, it is equivalent to replace the numerator in equation (23) with the shadow price of the transition equation of cumulative global emissions (12) at time

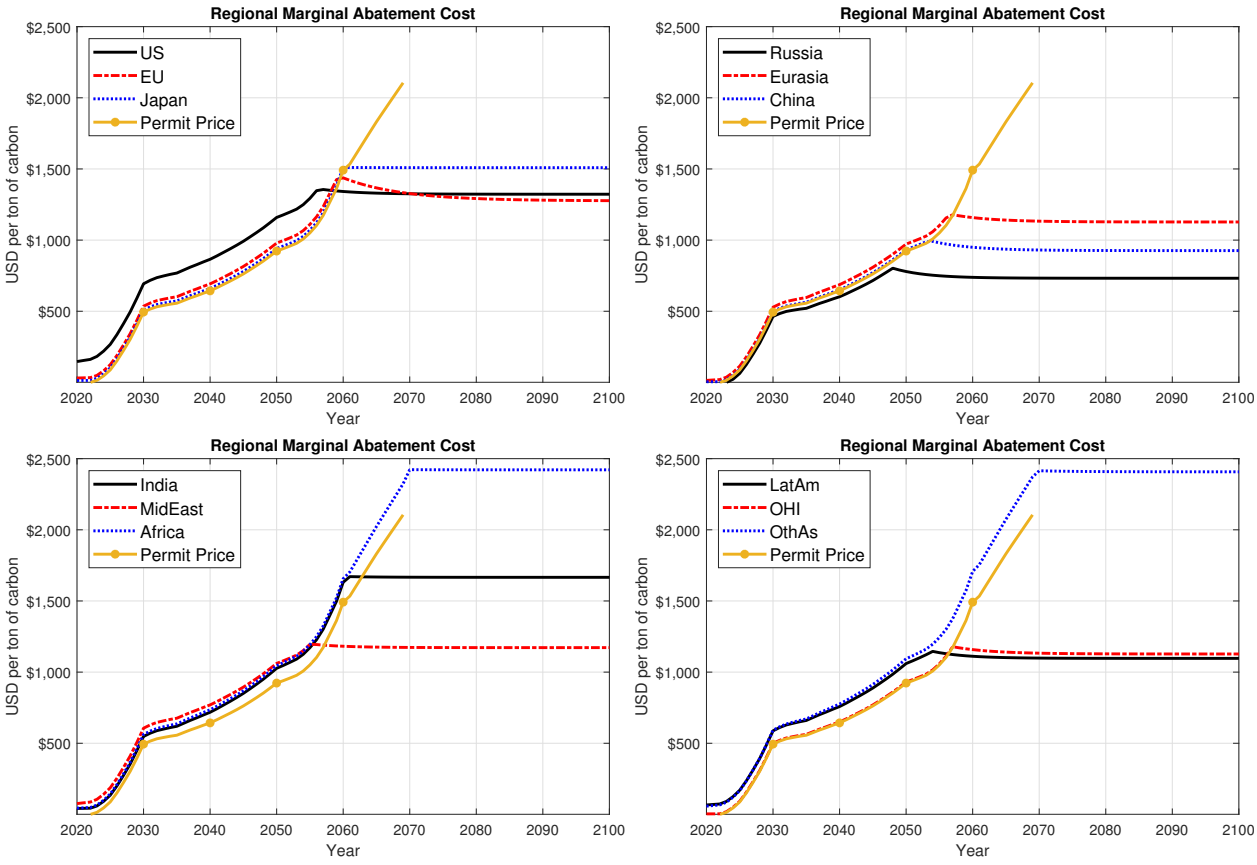

Figure 3: Simulation results of regional MAC under the baseline emission cap scenario.

emissions are measured in gigatonnes of carbon (GtC) and capital is measured in trillions of USD, our SCC is measured in monetary unit of 2020 USD per ton of carbon. [25]

The simulation results confirm the relationship between the regional SCC, MAC, and permit prices in a multi-region economy with a global ETS, as explored in Section 3. Figure 4 demonstrates that, when a region's net emissions are strictly positive, the regional SCC is exactly equal to the gap between the regional MAC and the permit price shown in Figure

t, and replace the denominator with the shadow price of the regional capital transition equation (5) for each region.

[25]The choice of discount rates has been a critical factor contributing to the gap in social cost of carbon estimates across different studies (Guo et al., 2006; Weitzman, 2013). Our concept of regional SCC differs from the definition in Nordhaus (2017), where the regional SCC is obtained by assuming that it is a fraction of the global SCC, with the share determined by the discounted value of regional output using an exogenous, constant discount rate. We verified numerically that our regional noncooperative SCC is equal to the present value of future climate damages in the region resulting from an additional unit of global emissions released in the current period, with our social discount rates $r_{i,t+1}$ defined endogenously with the following formula:

$$r_{i,t+1} = \frac{u'(c_{i,t})}{\beta u'(c_{i,t+1})} - 1,$$

where $c_{i,t}$ are the optimal per-capita consumptions.

3.[26] For example, in 2050, the MAC for the US is \$1,159 per ton of carbon, the permit price is \$923, and their difference is exactly equal to the regional SCC of the US, \$236. Russia is an exceptional case with a negative SCC in our simulation, suggesting that global warming creates benefits rather than causing climate damages in Russia, a result heavily influenced by the climate damage parameters calibrated using projections from Burke et al. (2018). Nevertheless, the relationship between the SCC, MAC, and permit price remains intact; for example, in 2040, the SCC for Russia is $-$\$41, which corresponds to the difference between the MAC (\$602) and the permit price (\$643). This explains why the MAC falls below the permit price starting in 2021, despite Russia having nonzero emissions until 2050. Among all the regions, the US has the highest SCC in the near term, at around \$199 per ton of carbon in 2030. However, the SCCs of Africa and non-OECD Asia are expected to experience substantial increases, reaching \$675 for Africa and \$599 for non-OECD Asia by the end of the century. Russia, with the lowest SCC, experiences a steady negative SCC, reaching (-\$88) per ton of carbon by the end of the century, indicating that it benefits from global warming throughout the entire period. Our results show considerable heterogeneity in the SCC across regions.

7.3 Effects of ETS Implementation

Next, we examine the economic and climate implications of the ETS implementation by comparing the global economy with and without the ETS regime, while maintaining the baseline emission caps in both economies. The top two panels of Figure 5 show that the ETS implementation results in slightly higher emissions and temperature increases compared to the case without the ETS. This pattern persists until 2043. This occurs because, under the ETS, regions with binding regional emission cap constraints now have the option to purchase permits from regions with less restrictive emission caps, fully exploiting the total amount of permits allowed at the global level. In contrast, without the ETS, regions with binding regional emission caps cannot utilize surplus emission permits from other regions, resulting in global net emissions that are lower than or equal to those in the ETS scenario over time. In the bottom two panels of Figure 5, we compare the MAC and the SCC using the US as an illustrative example. The MAC of the US economy without the ETS is higher until 2056, reflecting that the US becomes a permit buyer under the ETS regime as MAC increases with increasing emission abatement.[27] The SCC comparison demonstrates that

[26] When regional net emissions are at zero, the regional SCC can be larger than the gap, $(\text{MAC}_i(E_i) - m^*)$, which could be negative, as shown in Figure 4.

[27] Before 2030, the emission control rate grows fast so the MAC of the US increases rapidly along time, but after 2030, the emission control rate grows slowly such that the improvement of emission abatement technology makes the MAC decline along time until 2042.

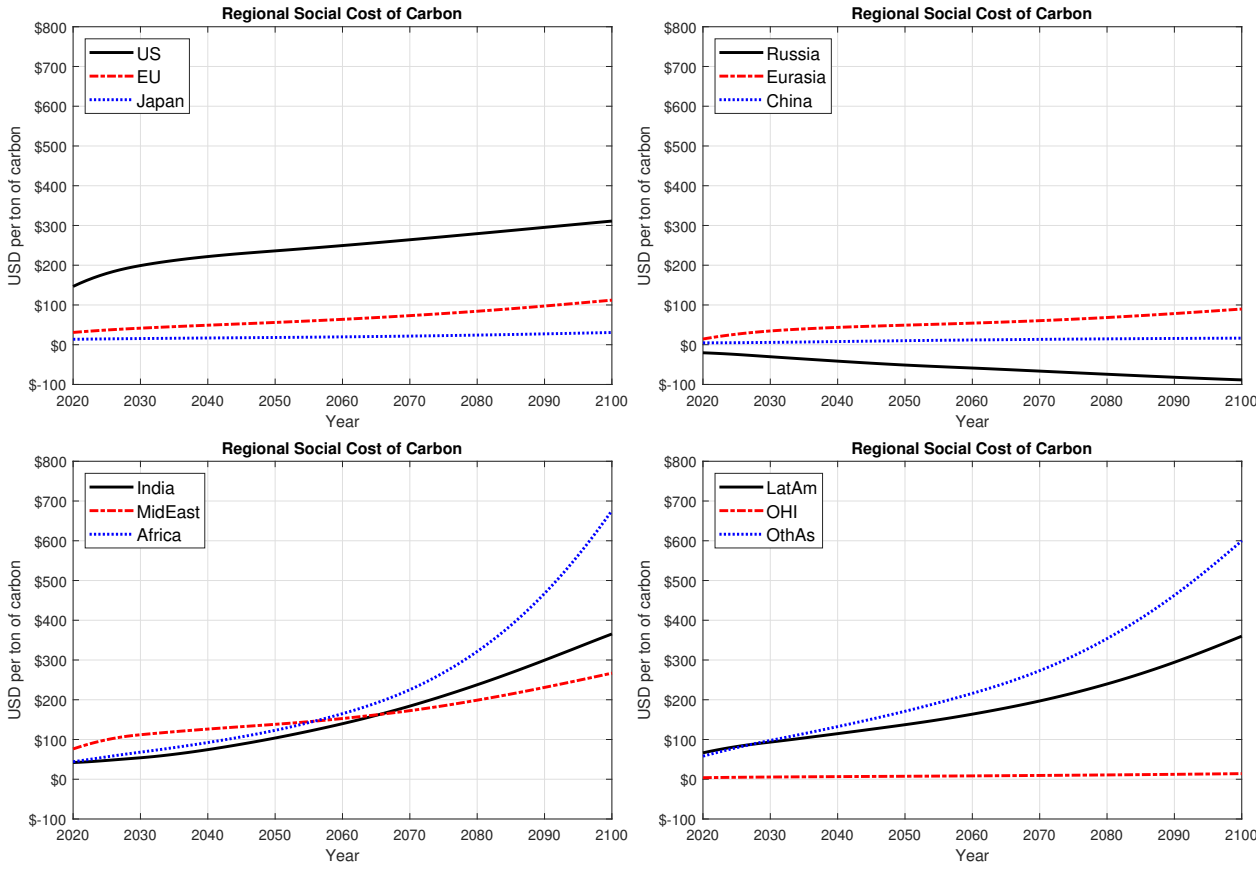

Figure 4: Simulation results of regional SCC under the baseline emission cap scenario.

the ETS has little impact on the regional SCC. This pattern holds for the other regions as well, as shown in Figure A.10. Since the regional noncooperative SCC is the present value of future climate damages in the region resulting from an additional unit of global emissions released in the current period, these results indicate that the ETS has little impact on either the marginal climate damages or our endogenous social discount rates.

What are the welfare implications of implementing the global ETS? To quantify these effects, we compute a compensating variation (CV) per capita associated with the ETS implementation. Specifically, the CV per capita for region i is computed by numerically solving the following equation:

$$W_{i,0}(\mathbf{c}_i^1 - CV) = W_{i,0}(\mathbf{c}_i^0), \tag{24}$$

where $\mathbf{c}_i^1 = (c_{i,0}^1, \cdots, c_{i,t}^1, \cdots, c_{i,T}^1)$ represents the vector of optimal consumption per capita under the ETS implementation, $\mathbf{c}_i^0 = (c_{i,0}^0, \cdots, c_{i,t}^0, \cdots, c_{i,T}^0)$ is the vector of optimal con-

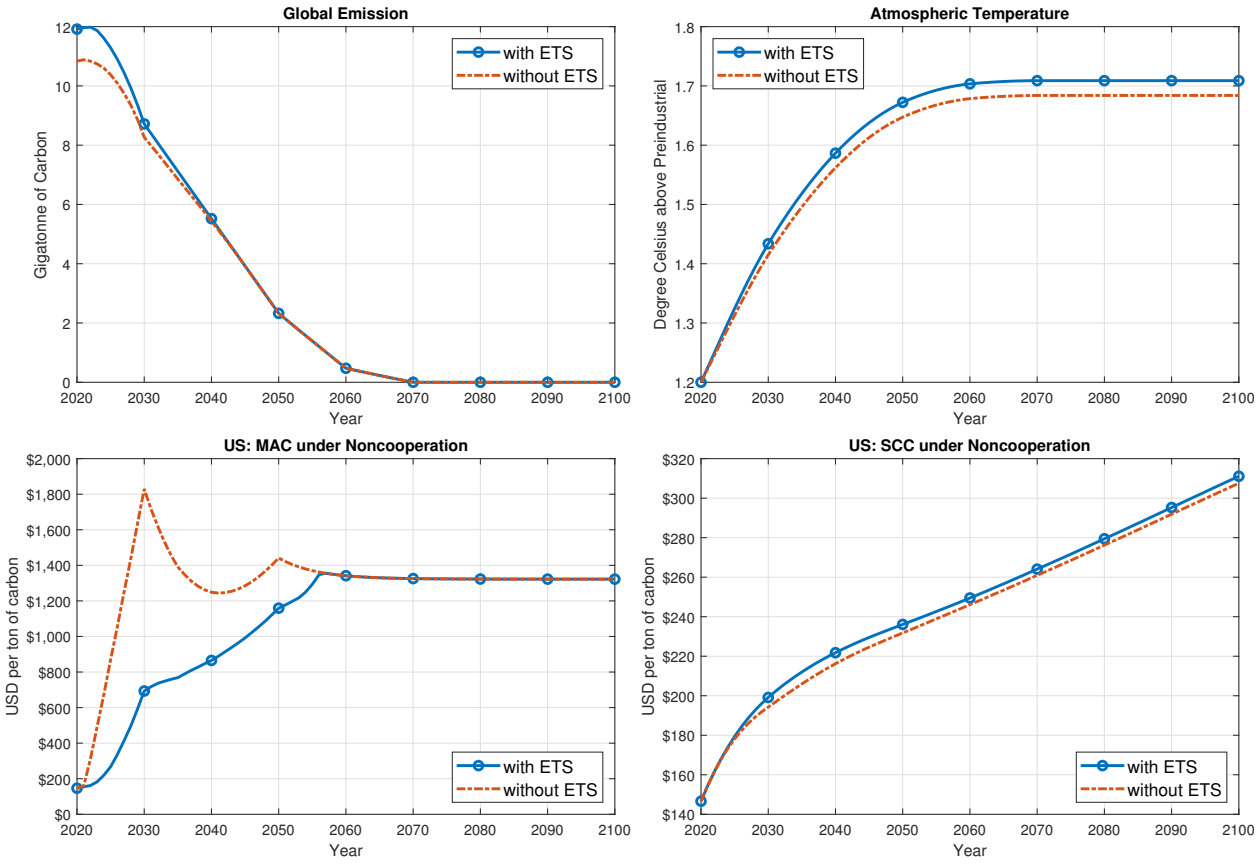

Figure 5: Comparative analysis: effects of the ETS implementation.

sumption per capita without the ETS implementation, and

$$W_{i,0}(\mathbf{c}_i) = \sum_{t=0}^{T} \beta^t u(c_{i,t}) L_{i,t}$$

is the social welfare associated with the vector of consumption per capita $\mathbf{c}_i = (c_{i,0}, \cdots, c_{i,t}, \cdots, c_{i,T})$ with the terminal time $T = 299$.

Table 1 shows welfare effects of the global ETS, measured by the CV per capita in 2020 USD, and its share (%) out of per capita consumption in each region at $t = 0$. The results reveal significant heterogeneity in welfare effects across regions: some regions experience welfare gains, with Russia benefiting the most, showing a CV per capita of \$552.75, equivalent to 6.699% of its per capita consumption. In contrast, other regions, including Africa, the Middle East, and non-OECD Asia, experience negative welfare effects. This outcome may seem counterintuitive, as one might expect an additional market mechanism (ETS) to enhance welfare by providing greater flexibility in managing emissions. It is important to note that a direct comparison of the noncooperative model with and without the ETS does not

provide a clear picture of the welfare effects of the ETS under the current baseline emission cap scenario, as the global net emissions and resulting climate damages differ across the two economies. Recall that, global average temperature is higher under ETS implementation in the baseline emission cap scenario, as shown in Figure 5. Therefore, the differences between $\mathbf{c}_i^1$ and $\mathbf{c}_i^0$ depend on both the global net emissions (and resulting climate damages) and the ETS implementation. As a result, some regions may experience additional climate damages due to higher temperatures, outweighing the benefits of lower abatement costs from permit purchases or additional profits from permit sales. This explains why some regions experience negative welfare effects from ETS implementation.

Table 1: Welfare effects of the ETS implementation: pre-emission cap adjustment.

	US	EU	Japan	Russia	Eurasia	China
CV per capita ($)	38.94	83.04	-0.03	552.75	53.18	42.90
CV per capita (%)	0.089	0.330	0.000	6.699	1.062	0.429
	India	MidEast	Africa	LatAm	OHI	OthAs
CV per capita ($)	22.94	-36.03	-5.40	66.68	109.69	-18.93
CV per capita (%)	1.469	-0.387	-0.354	1.001	0.317	-0.806

To isolate the impact of the ETS, we adjust the emission cap $\overline{E}_{i,t}$ in the noncooperative model with the ETS to $\overline{E}'_{i,t}$, which is the optimal level of net emissions obtained from the noncooperative model with the emission caps $\overline{E}_{i,t}$ but without the ETS. We then compare economies with and without the ETS under the emission cap $\overline{E}'_{i,t}$, ensuring two economies have the same pathways of global net emissions and temperature. Table 2 shows that the welfare impacts of the global ETS are strictly positive for all regions, irrespective of whether they are permit sellers or buyers, with considerable heterogeneity in the magnitude of these effects across the regions. For example, in the United States, the CV per capita is $116.18, which is a relatively small fraction of per capita consumption (0.267%). Among all regions, Russia still experiences the largest welfare improvement, with a CV per capita of $235.17, equivalent to 2.850% of its per capita consumption, though its welfare gains are smaller than in the pre-adjustment analysis. This is because Russia, a country with a negative SCC, benefits from higher temperatures, meaning that its welfare gains in the pre-adjustment analysis reflect both climate-induced benefits and ETS implementation. Conversely, Africa and non-OECD Asia experience the smallest welfare gains from the global ETS, indicating that additional climate damages from higher temperatures contributed to the negative welfare effects observed in the pre-adjustment analysis. Overall, the results in the post-adjustment analysis highlight that the principle of gains from trade applies to emissions trading as well,

driven by efficiency gains achieved through the reallocation of emission abatement efforts across regions.

Table 2: Welfare effects of the ETS implementation: post-emission cap adjustment.

	US	EU	Japan	Russia	Eurasia	China
CV per capita ($)	116.18	100.26	38.60	235.17	57.49	34.62
CV per capita (%)	0.267	0.399	0.136	2.850	1.148	0.346
	India	MidEast	Africa	LatAm	OHI	OthAs
CV per capita ($)	33.34	42.73	16.82	75.30	100.63	12.40
CV per capita (%)	2.135	0.459	1.103	1.130	0.291	0.529

8 Alternative Policy Simulations

Our model framework allows flexibility to explore alternative policy simulations. Recognizing that the actual implementation of a global ETS requires substantial international commitment, we consider two alternative policy scenarios to gain additional insights. First, we examine a partial ETS in which a major player in the world economy—the United States—does not participate, and the ETS operates among the remaining regions. Second, we analyze alternative net-zero pathways that vary in the stringency of global emission reduction commitments.

8.1 Partial ETS: US Non-participation

Recent political developments under the Trump administration have indicated that the United States is unlikely to participate in international cooperation aimed at mitigating global emissions in the near term. In light of this potential fragmentation of global climate cooperation, it is useful to numerically examine the economic and environmental consequences of a partial ETS. To this end, we simulate a scenario in which the United States refrains from any form of climate action—neither enforcing its emission cap nor participating in the ETS—while the remaining 11 regions continue to operate a cap-and-trade system.

Figure 6 compares the key outcomes under the baseline ("full ETS") and the partial ETS scenarios. As intuitively expected, US non-participation leads to a substantial increase in global emissions and a corresponding rise in global temperature, reaching 1.83 degrees Celsius—about 0.12 degrees Celsius higher than in the baseline. Under the partial ETS scenario, the US MAC is equal to its SCC which rises to $336 by 2100 due to higher global

average temperatures.

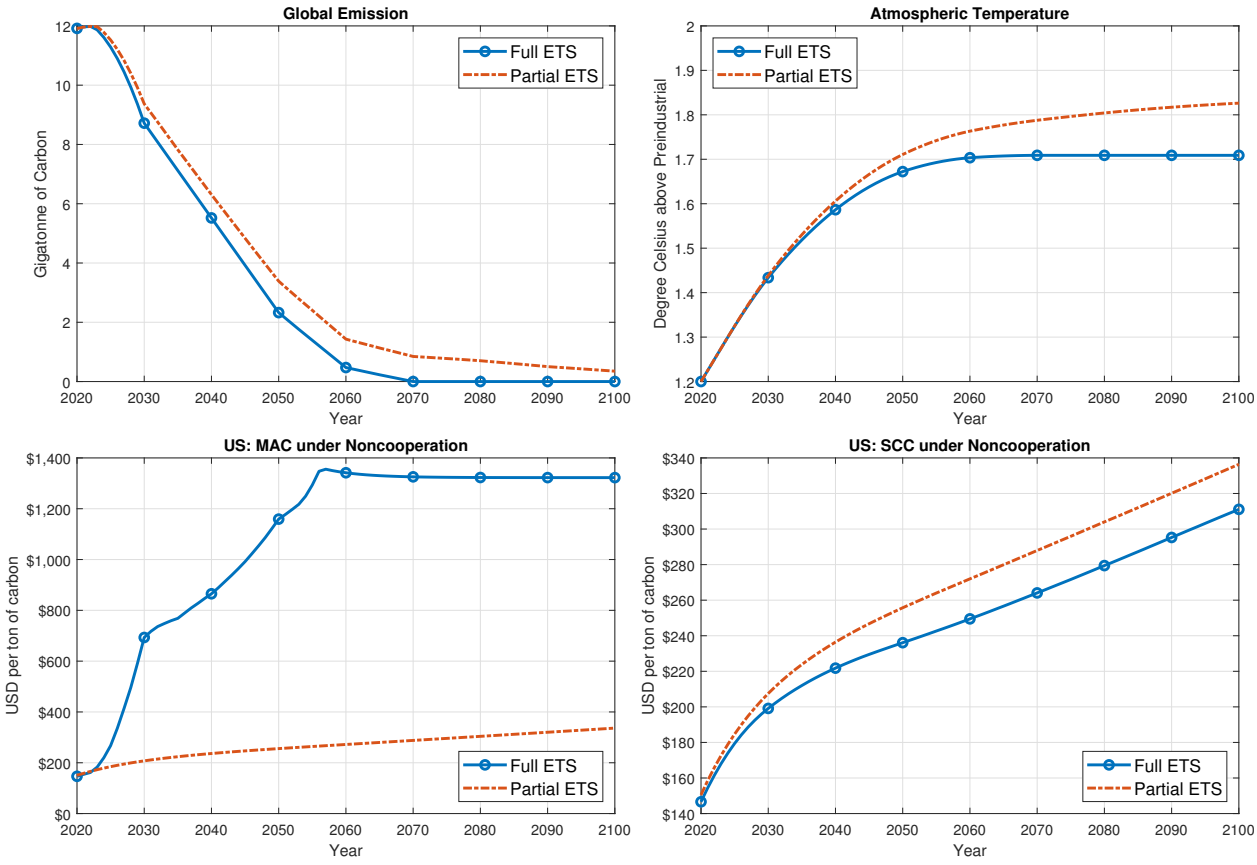

Figure 6: Comparative analysis: effects of US non-participation in the global ETS

Table 3 shows welfare effects of the US non-participation by comparing the partial ETS to the full ETS, further illustrating the distributional effects of fragmented climate cooperation. The United States experiences a significant welfare gain, with CV per capita of $565—approximately 1.3% of per capita consumption—reflecting its reduced abatement burden and the low level of MACs as shown in the figure above. On the other hand, the other regions (except for Russia) all experience significant welfare losses, ranging from -3.8% (MidEast) to -0.01% (OHI) of per capita consumption, as they bear the costs of both higher climate damages and continued emission constraints under the ETS. Russia is the only exception among the participating regions, experiencing welfare gains because higher global average temperatures are expected to benefit its economy, as noted earlier. Overall, this exercise underscores the critical importance of sustained and collective international commitment to climate mitigation, given the strong incentives for free-riding under noncooperative settings.

Table 3: Welfare effects of US non-participation in the global ETS

	US	EU	Japan	Russia	Eurasia	China
CV per capita ($)	564.96	-54.00	-115.07	105.06	-129.73	-10.15
CV per capita (%)	1.309	-0.215	-0.404	1.226	-2.561	-0.103
	India	MidEast	Africa	LatAm	OHI	OthAs
CV per capita ($)	-28.94	-327.27	-52.56	-121.99	-3.23	-79.91
CV per capita (%)	-1.867	-3.793	-3.409	-1.966	-0.009	-3.378

8.2 Net Zero Emission Scenarios

Along with the baseline emission cap scenario, we analyze simulation results for the noncooperative model with alternative emission cap paths, defined by the net zero emission targets in 2050, 2070, and 2090, where all regions achieve net zero emissions by the specified year. The top-left and top-right panels in Figure 7 display the emission permit prices and expected temperature increases under different emission cap scenarios. Under the net zero 2050 scenario, which is the most strict emission cap schedule, the emission permit price reaches $1,621 per ton of carbon in 2049, and the temperature rise is restricted to 1.62 degrees Celsius by the end of this century. Net zero 2070 and net zero 2090 are more relaxed scenarios, leading to permit prices at $616 and $446 per ton of carbon in 2049, respectively. In these scenarios, the temperature rise by the end of the century is expected to reach 1.80 degrees Celsius and 1.99 degrees Celsius above the pre-industrial level, respectively. This result shows that the global target of restricting the temperature rise to 1.5 degrees Celsius is unattainable in a noncooperative world, even under the most restrictive net zero 2050 scenario, suggesting that stronger measures are needed to effectively regulate global emissions.

The bottom-left and bottom-right panels in Figure 7 show the regional MAC and SCC, taking the US as an example. The comparison of the regional SCC and MAC for all other regions are available in Appendix A.4.4, which show the same patterns as the US. Our results show that stricter emission caps lead to higher MACs. Specifically, the MAC of the US under the net zero 2050 scenario can reach up to $1,493 per ton of carbon in 2048, compared to the peak of $1,322 in 2082 under the net zero 2090 scenario. This is because more rigorous emission caps imposed on each region entail additional abatement efforts, resulting in a higher MAC. We also find that more stringent emission caps result in a smaller SCC: the SCC of the US is $225 per ton of carbon in 2050 in the net zero 2050 scenario, while it is $270 in 2050 in the net zero 2090 scenario. This is because the permit price in the net zero 2050 scenario grows more quickly over time and even faster than the MAC.

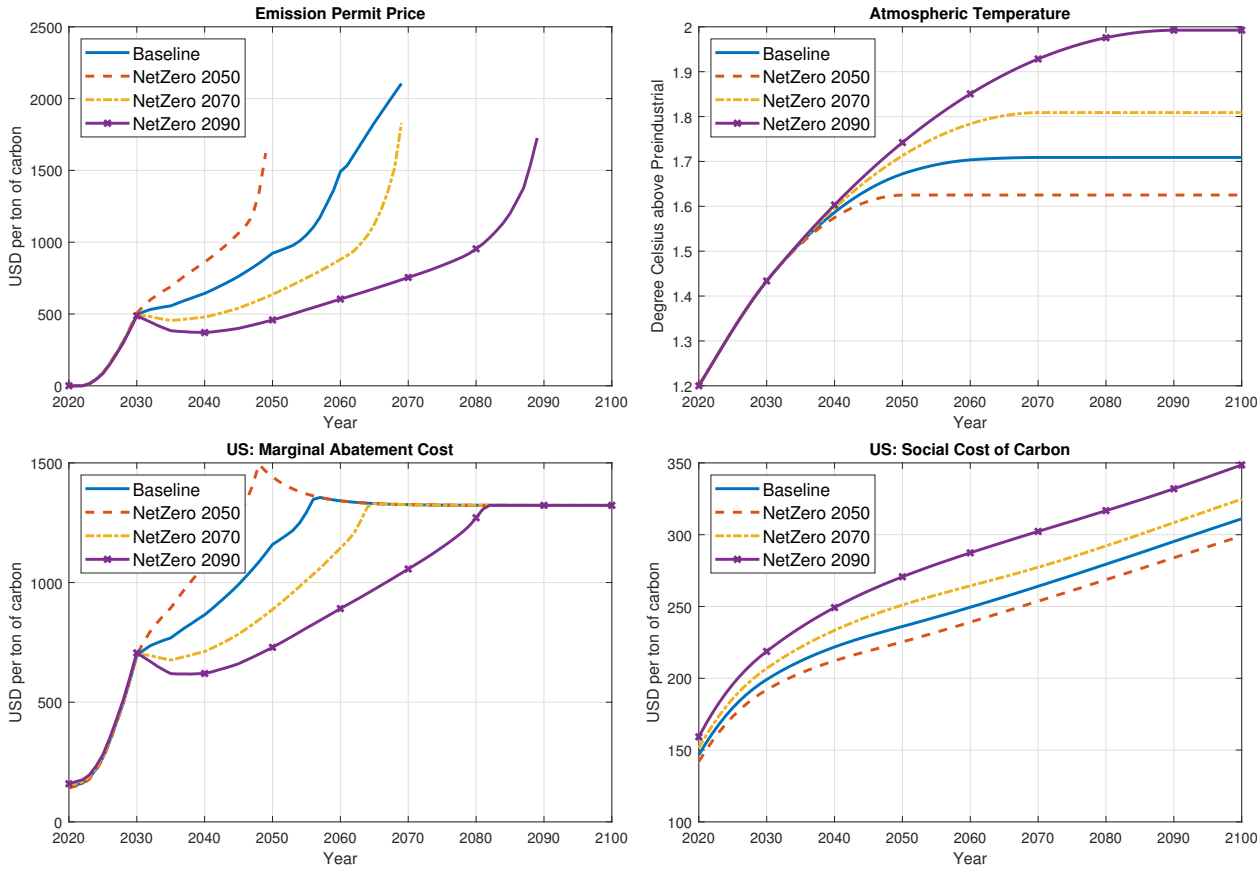

Figure 7: Sensitivity analysis: alternative emission cap scenarios.

9 Sensitivity Analysis

Lastly, recognizing that climate damages and emission abatement costs are key drivers of our model outcomes, including permit prices, MAC, and the SCC, we conduct sensitivity analyses on the parameters for climate damages ($\pi_{1,i}$, $\pi_{2,i}$) and emission abatement ($b_{1,i}$, $b_{2,i}$, $b_{3,i}$, $b_{4,i}$).

9.1 Climate Damage Parameters

. While we incorporate climate damage projections from Burke et al. (2018) as our baseline model simulation, we additionally consider projections from Kahn et al. (2021) and Nordhaus (2010a). Specifically, we calibrate the climate damage parameters to match the projections from Kahn et al. (2021) and directly adopt the parameters from Nordhaus (2010a). Figure 8 demonstrates the key economic and climate outcomes under different climate damage assumptions. The baseline climate damage parameters from Burke et al. (2018) result in slightly lower emission permit prices, reaching \$2,105 by 2069, compared to \$2,322 under

the damage parameters estimated from Kahn et al. (2021) and $2,334 under the damage parameters from Nordhaus (2010a). With the same emission cap constraints imposed, the global temperature outcomes remain unaffected despite variations in the damage parameters. For the US, the baseline climate damage estimation from Burke et al. (2018) leads to higher MAC and higher SCC, indicating that the baseline marginal climate damages are relatively higher than those projected by Kahn et al. (2021) and Nordhaus (2010a). However, regional heterogeneity exists; for example, Russia experiences negative SCC under the baseline parameter values, while experiencing small but positive SCC under the parameter values estimated from Kahn et al. (2021) and Nordhaus (2010a). See Appendix A.4.5 for a comparison across all 12 regions.

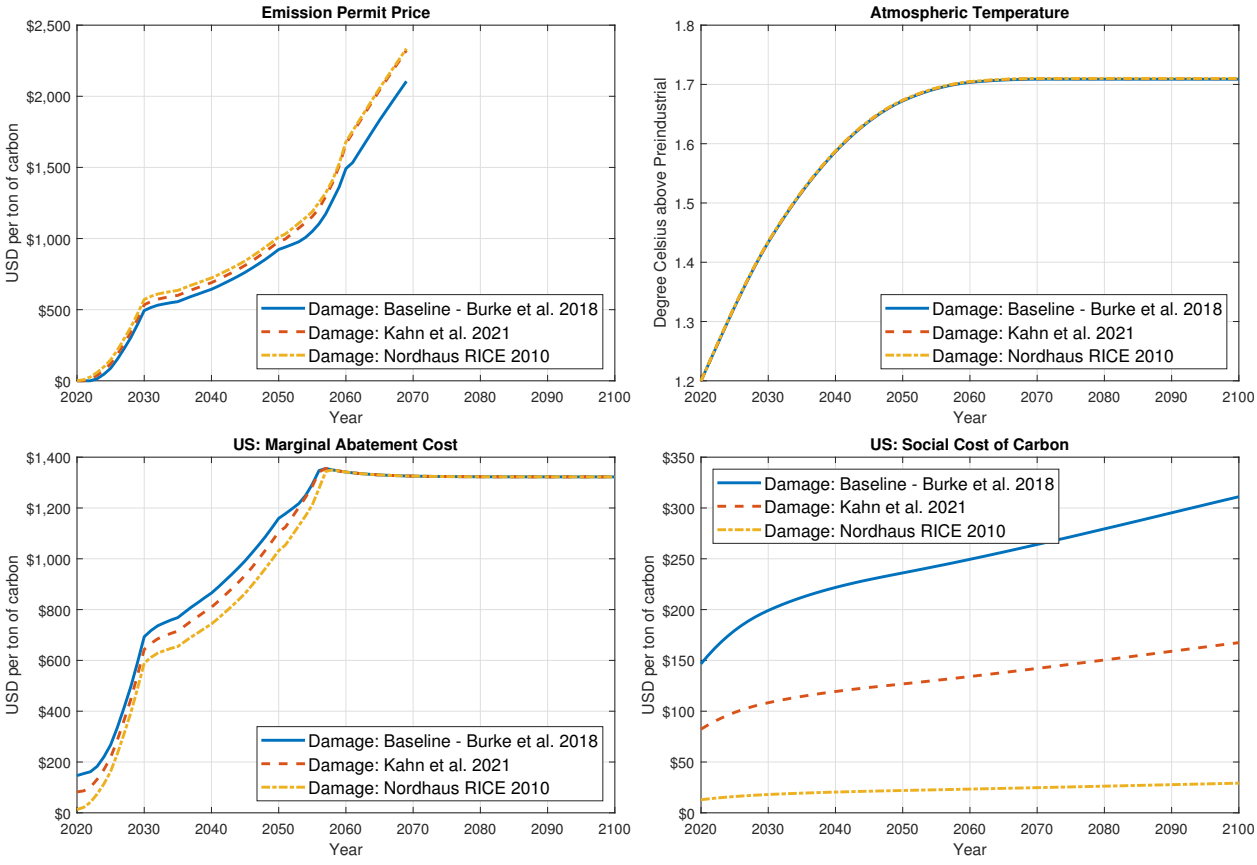

Figure 8: Sensitivity analysis: alternative climate damage parameters.

9.2 Abatement Cost Parameters

For our sensitivity analysis of the emission abatement cost parameters, we consider the parameter values from Nordhaus (2010a) in addition to the baseline parameter values calibrated from Ueckerdt et al. (2019), both of which share the same functional form of abatement cost.

As shown in Figure 9, the permit price rises to $1,717 by 2069 under the abatement cost estimate of Nordhaus (2010a), approximately 81% of the permit price projected under the baseline scenario. Despite the lower permit price, the global temperature increase remains similar to the baseline simulation, reaching 1.70 degrees Celsius by the end of the century, due to the emission cap constraints. The lower emission permit price under the abatement cost estimate of Nordhaus (2010a) reflects lower MAC, as illustrated with the US case in Figure 9, with similar patterns observed across most regions (see Appendix A.4.6). Lastly, the SCC is also lower under Nordhaus (2010a) parameters, with the SCC of the US reaching $102 by 2100—just 33% of the baseline scenario.

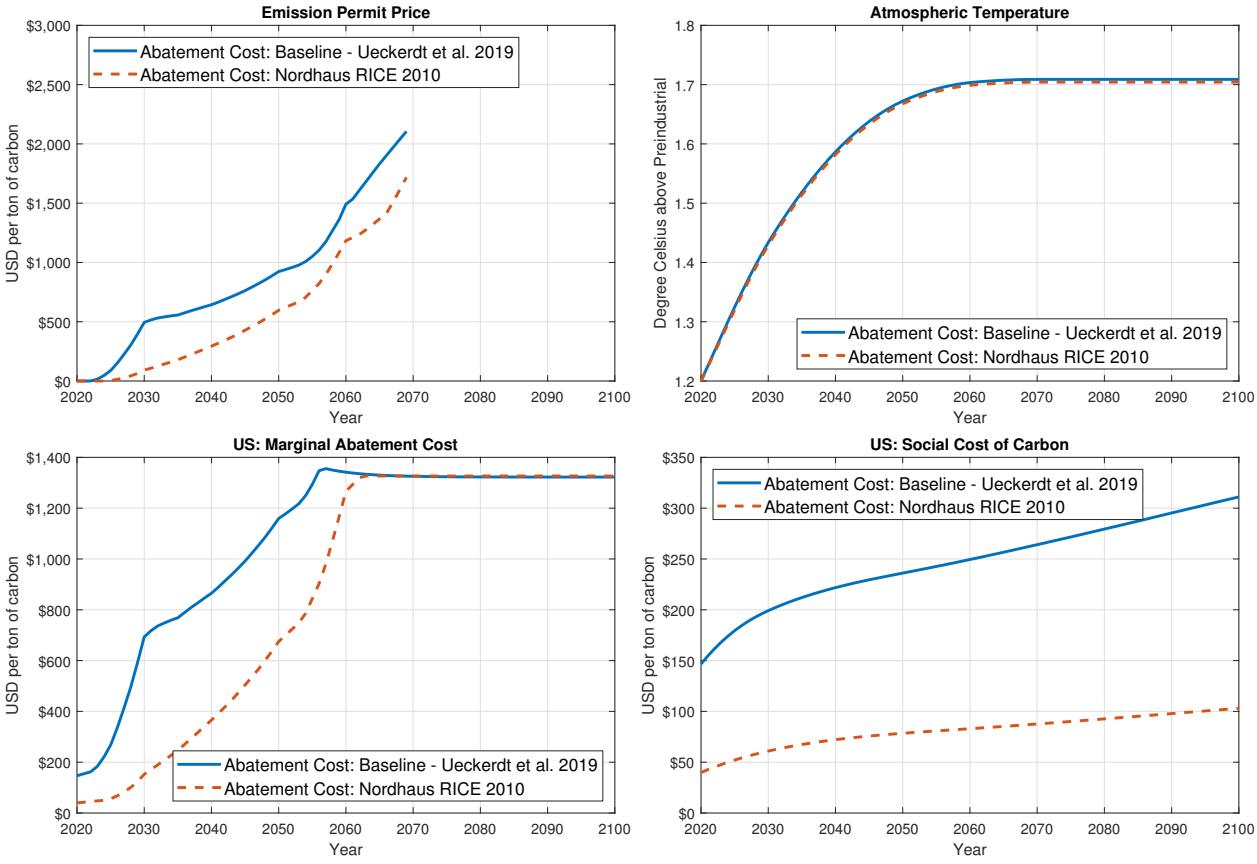

Figure 9: Sensitivity analysis: alternative abatement cost parameters

10 Conclusion

In this work, we build a dynamic multi-region model of climate and the economy with a global emission cap-and-trade system. In our integrated assessment framework, regions participating in a global or partial ETS are allocated emission caps in line with the emission

targets of the NDCs and net zero commitments, as established under the Paris Agreement and the Glasgow Pact. We solve for the market prices of emission permits under the dynamic Nash equilibrium in a noncooperative setting among the participating regions. The permit prices are endogenously determined by demand and supply of emission permits in the permits market, reflecting regional heterogeneity in future productivity growth, abatement technologies, climate damage, and population growth. For strictly positive emissions, we show both theoretically and numerically that the regional SCC is equal to the difference between the regional MAC and the market price of permits for regions participating in the ETS.

This work has several policy implications. First, our results indicate that the current global target of restricting the global temperature rise to 1.5 degrees Celsius above pre-industrial level by 2100 is unattainable under noncooperation, with the current emission commitments outlined in the Paris Agreement and the Glasgow Pact. Our findings suggest that more stringent emission reduction targets and global cooperation are needed to curb the trend of rising global temperature. Second, our baseline simulation shows that the current emission commitments lead to excess emission permit supply in the initial years, resulting in permit prices of zero. This finding suggests that effective implementation of the global ETS requires stricter emission caps so that the global supply of permits does not exceed the global demand of permits. Third, we demonstrate that an ETS is not a perfect substitute for a carbon tax; rather, the two instruments are complementary and can be jointly employed to enhance policy efficiency. Finally, our numerical analysis highlights the strong free-rider incentives in a partial ETS, illustrating why achieving sustained global cooperation in carbon mitigation remains a major challenge.

11 Declaration of generative AI and AI-assisted technologies in the writing process

During the preparation of this work, the authors used generative AI (ChatGPT) in order to improve the manuscript's readability during the revision process. After using this tool/service, the authors reviewed and edited the content as needed and take full responsibility for the content of the published article.

References

Ambec, S., Esposito, F., and Pacelli, A. (2024). The economics of carbon leakage mitigation policies. *Journal of Environmental Economics and Management*, page 102973.

Arias, P., Bellouin, N., Coppola, E., Jones, R., Krinner, G., Marotzke, J., Naik, V., Palmer, M., Plattner, G.-K., Rogelj, J., et al. (2021). Climate change 2021: The physical science basis. contribution of working group i to the sixth assessment report of the intergovernmental panel on climate change; technical summary.

Baldwin, E., Cai, Y., and Kuralbayeva, K. (2020). To build or not to build? capital stocks and climate policy. *Journal of Environmental Economics and Management*, 100(Article 102235).

Banzhaf, H. S. and Chupp, B. A. (2012). Fiscal federalism and interjurisdictional externalities: New results and an application to us air pollution. *Journal of Public Economics*, 96(5-6):449–464.

Barnett, M., Brock, W., and Hansen, L. P. (2020). Pricing Uncertainty Induced by Climate Change. *The Review of Financial Studies*, 33(3):1024–1066.

Bauer, N., Baumstark, L., and Leimbach, M. (2012). The REMIND-R model: the role of renewables in the low-carbon transformation—first-best vs. second-best worlds. *Climatic Change*, 114(1):145–168.

Böhringer, C., Fischer, C., and Rosendahl, K. E. (2014). Cost-effective unilateral climate policy design: Size matters. *Journal of Environmental Economics and Management*, 67(3):318–339.

Borenstein, S., Bushnell, J., Wolak, F. A., and Zaragoza-Watkins, M. (2019). Expecting the Unexpected: Emissions Uncertainty and Environmental Market Design. *American Economic Review*, 109(11):3953–3977.

Bosetti, V., Carraro, C., Galeotti, M., Massetti, E., and Tavoni, M. (2006). Witch a world induced technical change hybrid model. *The Energy Journal*, 27:13–37.

Bosetti, V., Carraro, C., and Massetti, E. (2009). Banking permits: Economic efficiency and distributional effects. *Journal of Policy Modeling*, 31(3):382–403. Climate Change and Energy Policy.

Brock, W. and Xepapadeas, A. (2017). Climate change policy under polar amplification. *European Economic Review*, 99:93–112.

Burke, M., Davis, W. M., and Diffenbaugh, N. S. (2018). Large potential reduction in economic damages under un mitigation targets. *Nature*, 557(7706):549–553.

Cai, Y. (2021). The role of uncertainty in controlling climate change. *Oxford Research Encyclopedia of Economics and Finance*.

Cai, Y., Brock, W., and Xepapadeas, A. (2023). Climate change impact on economic growth: Regional climate policy under cooperation and noncooperation. *Journal of the Association of Environmental and Resource Economists*, 10(3):569–605.

Carbone, J. C., Helm, C., and Rutherford, T. F. (2009). The case for international emission trade in the absence of cooperative climate policy. *Journal of environmental economics and management*, 58(3):266–280.

De Cian, E. and Tavoni, M. (2012). Do technology externalities justify restrictions on emission permit trading? *Resource and Energy Economics*, 34(4):624–646.

den Elzen, M. G. J., Dafnomilis, I., Forsell, N., Fragkos, P., Fragkiadakis, K., HÃ¶hne, N., Kuramochi, T., Nascimento, L., Roelfsema, M., van Soest, H., and Sperling, F. (2022). Updated nationally determined contributions collectively raise ambition levels but need strengthening further to keep paris goals within reach. *Mitigation and Adaptation Strategies for Global Change*, 27(5):33.

Dietz, S., van der Ploeg, F., Rezai, A., and Venmans, F. (2021). Are Economists Getting Climate Dynamics Right and Does It Matter? *Journal of the Association of Environmental and Resource Economists*, 8(5):895–921.

Dietz, S. and Venmans, F. (2019). Cumulative carbon emissions and economic policy: in search of general principles. *Journal of Environmental Economics and Management*, 96:108–129.

Doda, B., Quemin, S., and Taschini, L. (2019). Linking permit markets multilaterally. *Journal of Environmental Economics and Management*, 98:102259.

Farrokhi, F. and Lashkaripour, A. (2021). Can trade policy mitigate climate change. *Unpublished Working Paper*.

Fernández-Villaverde, J., Gillingham, K. T., and Scheidegger, S. (2025). Climate change through the lens of macroeconomic modeling. *Annual Review of Economics*, 17(Volume 17, 2025):125–150.

Fischer, C. and Springborn, M. (2011). Emissions targets and the real business cycle: Intensity targets versus caps or taxes. *Journal of Environmental Economics and Management*, 62(3):352–366.

Fowlie, M. and Muller, N. (2019). Market-based emissions regulation when damages vary across sources: What are the gains from differentiation? *Journal of the Association of Environmental and Resource Economists*, 6(3):593–632.

Fowlie, M., Reguant, M., and Ryan, S. P. (2016). Market-based emissions regulation and industry dynamics. *Journal of Political Economy*, 124(1):249–302.

Fowlie, M. L. and Reguant, M. (2022). Mitigating emissions leakage in incomplete carbon markets. *Journal of the Association of Environmental and Resource Economists*, 9(2):307–343.

Fuss, S., Flachsland, C., Koch, N., Kornek, U., Knopf, B., and Edenhofer, O. (2018). A framework for assessing the performance of cap-and-trade systems: insights from the european union emissions trading system. *Review of Environmental Economics and Policy*.

Golosov, M., Hassler, J., Krusell, P., and Tsyvinski, A. (2014). Optimal taxes on fossil fuel in general equilibrium. *Econometrica*, 82(1):41–88.

Goulder, L. H., Hafstead, M. A., and Dworsky, M. (2010). Impacts of alternative emissions allowance allocation methods under a federal cap-and-trade program. *Journal of Environmental Economics and management*, 60(3):161–181.

Goulder, L. H., Long, X., Lu, J., and Morgenstern, R. D. (2022). China's unconventional nationwide co2 emissions trading system: Cost-effectiveness and distributional impacts. *Journal of Environmental Economics and Management*, 111:102561.

Goulder, L. H. and Parry, I. W. (2008). Instrument choice in environmental policy. *Review of environmental economics and policy*.

Goulder, L. H. and Schein, A. R. (2013). Carbon taxes versus cap and trade: a critical review. *Climate Change Economics*, 4(03):1350010.

Guo, J., Hepburn, C. J., Tol, R. S., and Anthoff, D. (2006). Discounting and the social cost of carbon: a closer look at uncertainty. *Environmental Science Policy*, 9(3):205–216.

Habla, W. and Winkler, R. (2018). Strategic delegation and international permit markets: Why linking may fail. *Journal of environmental economics and management*, 92:244–250.

Hahn, R. W. and Stavins, R. N. (2011). The effect of allowance allocations on cap-and-trade system performance. *Journal of Law and Economics*, 54:S267–S294. A-73.

Hambel, C., Kraft, H., and Schwartz, E. (2021). The social cost of carbon in a non-cooperative world. *Journal of International Economics*, 131:103490.

Harstad, B. and Eskeland, G. S. (2010). Trading for the future: Signaling in permit markets. *Journal of public economics*, 94(9-10):749–760.

Hitzemann, S. and Uhrig-Homburg, M. (2018). Equilibrium price dynamics of emission permits. *Journal of Financial and Quantitative Analysis*, 53(4):1653–1678.

Holland, S. P. and Yates, A. J. (2015). Optimal trading ratios for pollution permit markets. *Journal of Public Economics*, 125:16–27.

Holtsmark, B. and Weitzman, M. L. (2020). On the effects of linking cap-and-trade systems for co 2 emissions. *Environmental and Resource Economics*, 75(3):615–630.

Holtsmark, K. and Midttømme, K. (2021). The dynamics of linking permit markets. *Journal of Public Economics*, 198:104406.

Iverson, T. and Karp, L. (2021). Carbon taxes and climate commitment with non-constant time preference. *The Review of economic studies*, 88(2):764–799.

Jaakkola, N. and Van der Ploeg, F. (2019). Non-cooperative and cooperative climate policies with anticipated breakthrough technology. *Journal of Environmental Economics and Management*, 97:42–66.

Jakob, M., Luderer, G., Steckel, J., Tavoni, M., and Monjon, S. (2012). Time to act now? assessing the costs of delaying climate measures and benefits of early action. *Climatic Change*, 114(1):79–99.

Kahn, M. E., Mohaddes, K., Ng, R. N., Pesaran, M. H., Raissi, M., and Yang, J.-C. (2021). Long-term macroeconomic effects of climate change: A cross-country analysis. *Energy Economics*, 104:105624.

Karp, L. and Traeger, C. (2024). Taxes versus quantities reassessed. *Journal of Environmental Economics and Management*, 125:102951.

Keohane, N. O. (2009). Cap and trade, rehabilitated: Using tradable permits to control u.s. greenhouse gases. *Review of Environmental Economics and Policy*, 3(1):42–62.

Keohane, N. O. and Olmstead, S. M. (2016). *Markets and the Environment*. Island Press, Washington, DC.

Levinson, A. (2023). Are developed countries outsourcing pollution? *Journal of Economic Perspectives*, 37(3):87–110.

Luderer, G., Bosetti, V., Jakob, M., Leimbach, M., Steckel, J. C., Waisman, H., and Edenhofer, O. (2012). The economics of decarbonizing the energy system—results and insights from the recipe model intercomparison. *Climatic Change*, 114:9–37.

Massetti, E. and Tavoni, M. (2012). A developing asia emission trading scheme (asia ets). *Energy Economics*, 34:S436–S443. The Asia Modeling Exercise: Exploring the Role of Asia in Mitigating Climate Change.

Mattauch, L., Matthews, H. D., Millar, R., Rezai, A., Solomon, S., and Venmans, F. (2020). Steering the Climate System: Using Inertia to Lower the Cost of Policy: Comment. *American Economic Review*, 110(4):1231–1237.

Matthews, H. D., Gillett, N. P., Stott, P. A., and Zickfeld, K. (2009). The proportionality of global warming to cumulative carbon emissions. *Nature*, 459(7248):829–832.

Mehling, M. A., Metcalf, G. E., and Stavins, R. N. (2018). Linking climate policies to advance global mitigation. *Science*, 359(6379):997–998.

Meinshausen, M., Lewis, J., McGlade, C., Gutschow, J., Nicholls, Z., Burdon, R., Cozzi, L., and Hackmann, B. (2022). Realization of paris agreement pledges may limit warming just below 2 C. *Nature*, 604(7905):304–309.

Meinshausen, M., Smith, S. J., Calvin, K., Daniel, J. S., Kainuma, M. L., Lamarque, J.-F., Matsumoto, K., Montzka, S. A., Raper, S. C., Riahi, K., et al. (2011). The rcp greenhouse gas concentrations and their extensions from 1765 to 2300. *Climatic change*, 109:213–241.

Montgomery, W. D. (1972). Markets in licenses and efficient pollution control programs. *Journal of Economic Theory*, 5(3):395–418.

Muller, N. Z. and Mendelsohn, R. (2009). Efficient pollution regulation: getting the prices right. *American Economic Review*, 99(5):1714–1739.

Newell, R. G. and Pizer, W. A. (2003). Regulating stock externalities under uncertainty. *Journal of environmental economics and management*, 45(2):416–432.

Nordhaus, W. (2010a). *Excel file for RICE model as of April 26, 2010*.

Nordhaus, W. (2014). *A question of balance: Weighing the options on global warming policies*. Yale University Press.

Nordhaus, W. D. (2007). To tax or not to tax: Alternative approaches to slowing global warming. *Review of Environmental Economics and Policy*, 1(1):26–44.

Nordhaus, W. D. (2010b). Economic aspects of global warming in a post-copenhagen environment. *Proceedings of the National Academy of Sciences*, 107(26):11721–11726.

Nordhaus, W. D. (2017). Revisiting the social cost of carbon. *Proceedings of the National Academy of Sciences*, 114(7):1518–1523.

Nordhaus, W. D. and Yang, Z. (1996). A regional dynamic general-equilibrium model of alternative climate-change strategies. *The American Economic Review*, pages 741–765.

Oates, W. E. (1999). An essay on fiscal federalism. *Journal of economic literature*, 37(3):1120–1149.

Ogawa, H. and Wildasin, D. E. (2009). Think locally, act locally: Spillovers, spillbacks, and efficient decentralized policymaking. *American Economic Review*, 99(4):1206–1217.

Perino, G., Willner, M., Quemin, S., and Pahle, M. (2022). The european union emissions trading system market stability reserve: does it stabilize or destabilize the market? *Review of Environmental Economics and Policy*, 16(2):338–345.

Samir, K. and Lutz, W. (2017). The human core of the shared socioeconomic pathways: Population scenarios by age, sex and level of education for all countries to 2100. *Global Environmental Change*, 42:181–192.

Schmalensee, R. and Stavins, R. N. (2017). Lessons learned from three decades of experience with cap and trade. *Review of Environmental Economics and Policy*.

Stavins, R. N. (1996). Correlated uncertainty and policy instrument choice. *Journal of Environmental Economics and Management*, 30(2):218–232.

Stavins, R. N. (2022). The relative merits of carbon pricing instruments: Taxes versus trading. *Review of Environmental Economics and Policy*, 16(1):62–82.

Strand, J. (2013). Strategic climate policy with offsets and incomplete abatement: Carbon taxes versus cap-and-trade. *Journal of Environmental Economics and Management*, 66(2):202–218.

Ueckerdt, F., Frieler, K., Lange, S., Wenz, L., Luderer, G., and Levermann, A. (2019). The economically optimal warming limit of the planet. *Earth System Dynamics*, 10(4):741–763.

van de Ven, D.-J., Mittal, S., Gambhir, A., Lamboll, R. D., Doukas, H., Giarola, S., Hawkes, A., Koasidis, K., Koberle, A. C., McJeon, H., Perdana, S., Peters, G. P., Rogelj, J., Sognnaes, I., Vielle, M., and Nikas, A. (2023). A multimodel analysis of post-glasgow climate targets and feasibility challenges. *Nature Climate Change*, 13(6):570–578.

van der Ploeg, F. and de Zeeuw, A. (2016). Non-cooperative and cooperative responses to climate catastrophes in the global economy: A north–south perspective. *Environmental and Resource Economics*, 65:519–540.

Weitzman, M. L. (1974). Prices vs. Quantities. *The Review of Economic Studies*, 41(4):477–491.

Weitzman, M. L. (2013). Tail-hedge discounting and the social cost of carbon. *Journal of Economic Literature*, 51(3):873–882.

Williams III, R. C. (2012). Growing state–federal conflicts in environmental policy: The role of market-based regulation. *Journal of Public Economics*, 96(11-12):1092–1099.

World Bank (2020). Total greenhouse gas emissions (kt of co2 equivalent).

Yang, Z. (2023). The Model Dimensionality and Its Impacts on the Strategic and Policy Outcomes in IAMs: the Findings from the RICE2020 Model. *Computational Economics*, 62(3):1087–1106.

Appendix for Online Publication

A.1 List of Parameters

Table A.1 lists the key parameters and their values.

Table A.1: Key parameters.

Parameter	Value	Description
1) Economic system parameters (from Nordhaus (2017))		
β	0.985	Annual discount factor
γ	1.45	Elasticity of marginal utility
α	0.3	Output elasticity of capital
δ	0.1	Annual depreciation rate of capital
2) Climate system parameters		
ζ	0.0021	Contribution rate of carbon emissions to temperature

Table A.2 lists the values of the baseline abatement cost parameters calibrated from Ueckerdt et al. (2019). The values of carbon intensity at annual time steps will be provided upon request.

Table A.2: Abatement cost parameters (baseline) calibrated from Ueckerdt et al. (2019)

	US	EU	Japan	Russia	Eurasia	China
$b_{1,i}$	0.462	0.477	0.750	0.292	0.347	0.328
$b_{2,i}$	2.859	2.670	2.011	2.499	3.243	2.822
$b_{3,i}$	9.920	5.832	2.492	7.625	7.966	7.189
$b_{4,i}$	0.182	0.114	0.2	0.2	0.168	0.168
	India	MidEast	Africa	LatAm	OHI	OthAs
$b_{1,i}$	0.594	0.455	0.665	0.286	0.347	0.602
$b_{2,i}$	2.802	2.574	3.636	3.828	3.243	3.995
$b_{3,i}$	6.336	11.205	6.558	11.496	7.966	6.518
$b_{4,i}$	0.2	0.2	0.2	0.2	0.168	0.163

Table A.3 lists the calibrated values of the climate damage parameters used in the baseline analysis.

Table A.3: Climate damage parameters (baseline) calibrated from Burke et al. (2018)

	US	EU	Japan	Russia	Eurasia	China
$\pi_{1,i}$	0.0842	0.0489	0.0090	-0.4169	0.2678	0.0003
$\pi_{2,i}$	0.0096	0.0011	0.0748	0.3094	0.0002	0.0008
	India	MidEast	Africa	LatAm	OHI	OthAs
$\pi_{1,i}$	0.0017	0.3595	0.1886	0.1801	0.0123	0.2161
$\pi_{2,i}$	0.3276	0.0088	0.0764	0.0030	0.0044	0.0224

Table A.4 lists the values of the TFP parameters calibrated from Burke et al. (2018).

Table A.4: TFP parameters calibrated from Burke et al. (2018)

	US	EU	Japan	Russia	Eurasia	China
$g_{i,0}$	0.0033	0.0089	0.0085	0.0170	0.0094	0.0345
d_i	0.0011	0.0010	0.0010	0.0154	0.0010	0.0308
	India	MidEast	Africa	LatAm	OHI	OthAs
$g_{i,0}$	0.0332	0.0093	0.0218	0.0134	0.0076	0.0221
d_i	0.0151	0.0010	0.0013	0.0010	0.0010	0.0062

A.2 List of Countries

Table A.5: List of countries for regional aggregation

Region	Constituent Countries
Africa	Algeria, Angola, Benin, Botswana, Burkina Faso, Burundi, Cameroon, Cape Verde, Central African Republic, Chad, Comoros, Democratic Republic of the Congo, Republic of the Congo, Cote d'Ivoire, Djibouti, Arab Republic of Egypt, Ethiopia, Gabon, Gambia, The Ghana, Guinea, Guinea-Bissau, Kenya, Lesotho, Libya, Madagascar, Mali, Mauritania, Mauritius, Morocco, Mozambique, Namibia, Niger, Rwanda, Senegal, Sierra Leone, South Africa, Sudan, Swaziland, Tanzania, Togo, Tunisia, Uganda, Zambia, Zimbabwe.
European Union[28].	Austria, Belgium, Bulgaria, Croatia, Czech Republic, Denmark, Finland, France, Germany, Greece, Hungary, Ireland, Italy, Latvia, Lithuania, Luxembourg, Netherlands, Poland, Portugal, Romania, Slovak Republic, Spain, Sweden, United Kingdom.
Eurasia	Albania, Armenia, Azerbaijan, Belarus, Bosnia and Herzegovina, Estonia, Georgia, Kazakhstan, Kyrgyz Republic, FYR Macedonia, Moldova, Serbia, Slovenia, Tajikistan, Turkey, Ukraine, Uzbekistan.
Latin America	Argentina, Bahamas, The Belize, Bolivia, Brazil, Chile, Colombia, Costa Rica, Cuba, Dominican Republic, Ecuador, El Salvador, Guatemala, Haiti, Honduras, Mexico, Nicaragua, Panama, Paraguay, Peru, Puerto Rico, Trinidad and Tobago, Uruguay.
Middle East	Cyprus, Islamic Republic of Iran, Iraq, Israel, Jordan, Lebanon, Oman, Qatar, Saudi Arabia, United Arab Emirates
Other Non-OECD Asia	Afghanistan, Bangladesh, Bhutan, Brunei Darussalam, Cambodia, Fiji, Indonesia, Malaysia, Mongolia, Nepal, Pakistan, Philippines, Samoa, Solomon Islands, Sri Lanka, Thailand, Vanuatu, Vietnam.
Other High-Income	Australia, Canada, Iceland, Republic of Korea, New Zealand, Norway, Switzerland.

[28]The current EU does not contain the United Kingdom, but in this paper we still assume the United Kingdom is in the EU for convenience.

A.3 Details about Calibration and Data

A.3.1 Calibration of the TCRE Climate System

Each of the four RCP scenarios (Meinshausen et al., 2011) — RCP 2.6, RCP 4.5, RCP 6, and RCP 8.5 — provide their pathways of emissions, atmospheric carbon concentration, radiative forcing, and atmospheric temperature anomaly. When we calibrate the contribution rate of carbon emissions on temperature, ζ, in a climate system, we use the pathways of emissions and atmospheric temperature anomaly of the four RCP scenarios. Figure A.1 shows that our calibrated TCRE climate system provides a very good projection of the atmospheric temperature anomaly (increase relative to pre-industrial levels) based on cumulative emissions only.

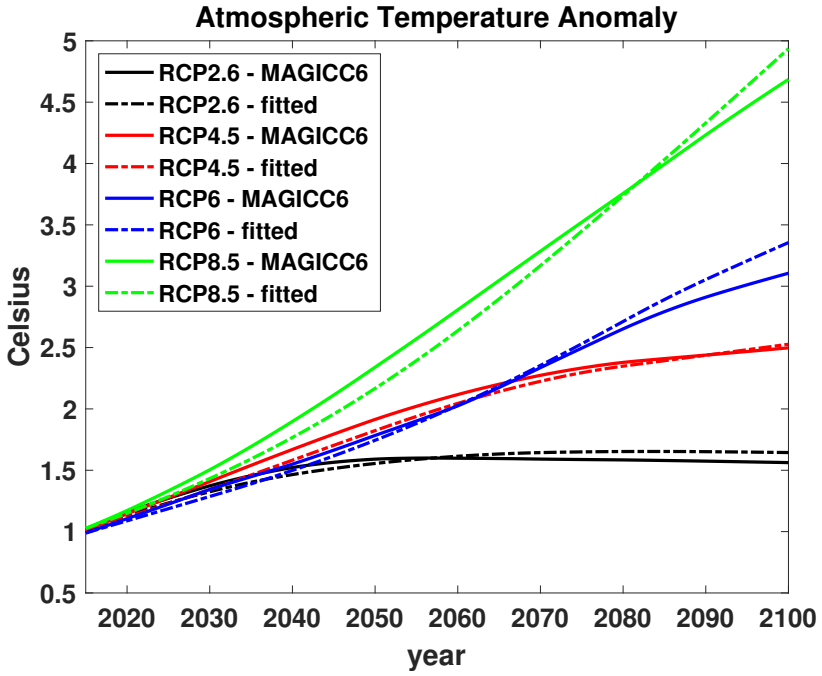

Figure A.1: Calibration of the TCRE climate system.

A.3.2 Calibration of Total Factor Productivity and Climate Damage

Figures A.2 and A.3 show that with our calibrated TFP and climate damage coefficients, the GDP per capita $y_{i,t}^{\text{NoCC}}$ or $y_{i,t}$ matches well with the projected data $y_{i,t}^{\text{BDD,NoCC}}$ or $y_{i,t}^{\text{BDD}}$ from Burke et al. (2018), respectively, for all regions.

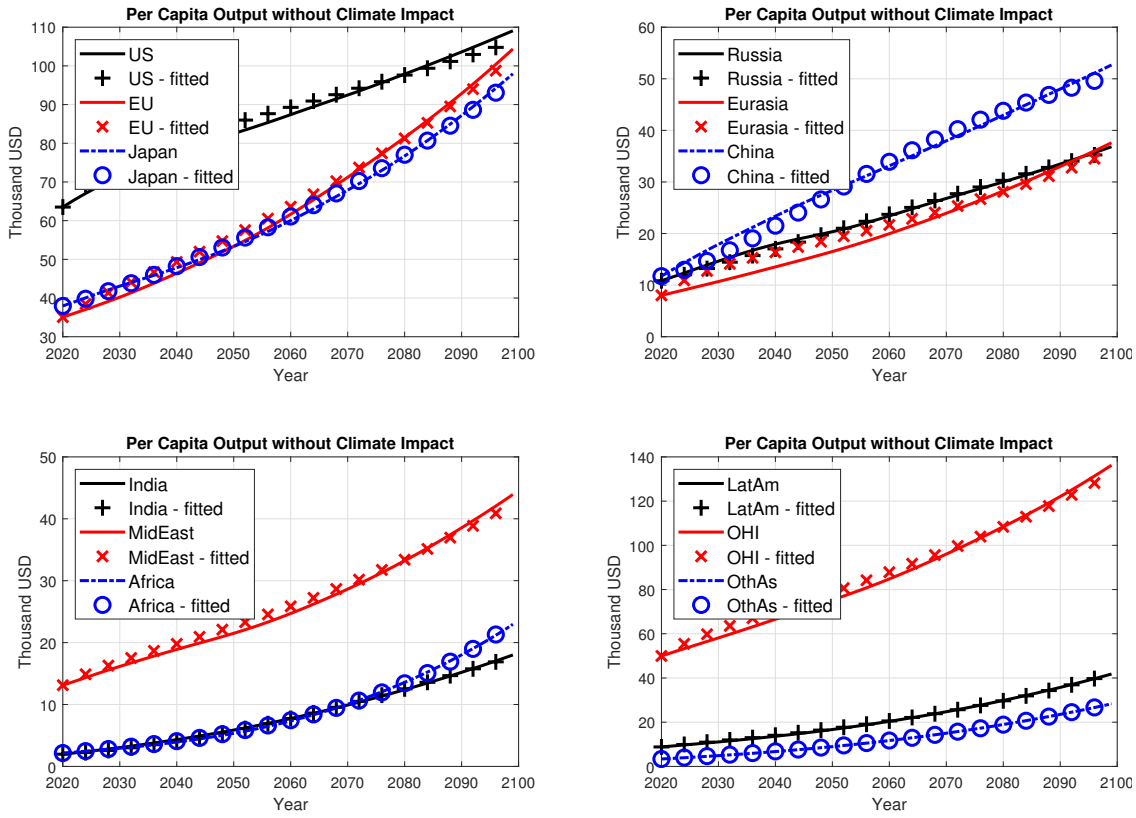

Figure A.2: Fitting GDP per capita under no climate impact. Lines represent GDP per capita under no climate impact from Burke et al. (2018); marks represent fitted GDP per capita.

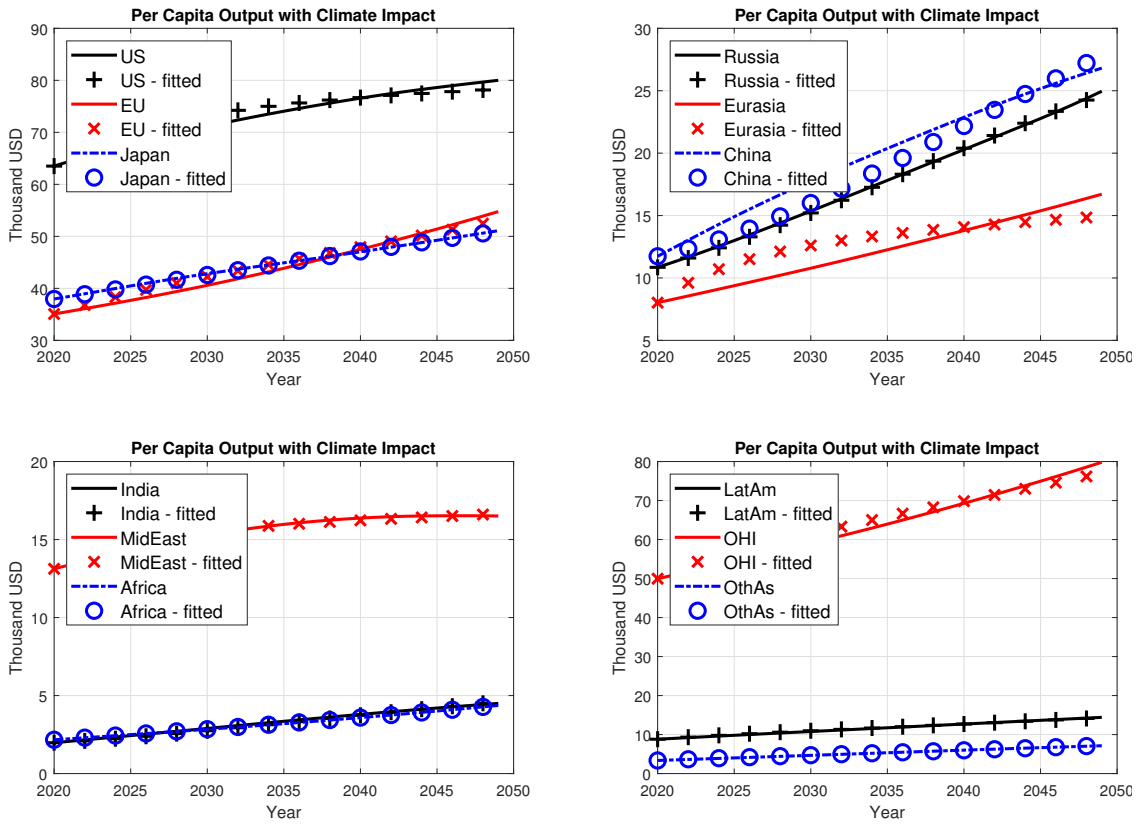

Figure A.3: Fitting GDP under climate impact. Lines represent the GDP per capita under the climate impact of RCP 4.5 from Burke et al. (2018); marks represent fitted values.

A.3.3 Calibration of Climate Damage from Kahn et al. (2021)

For sensitivity analysis on climate damage parameters in Section 9.1, we calibrate the climate damage parameters $\pi_{1,i}$ and $\pi_{2,i}$ by considering projections on GDP loss across different climate scenarios in Kahn et al. (2021), which shows the percentage loss in GDP per capita by 2030, 2050, and 2100 under the RCP 2.6 and RCP 8.5 scenarios for China, EU, India, Russia, and the US. We use their method and data to project the percentage loss in GDP per capita ($\Delta_{i,t}^{\text{RCP26}}$ and $\Delta_{i,t}^{\text{RCP85}}$) every year from 2020 to 2114 under the RCP 2.6 and RCP 8.5 scenarios for each of our 12 regions, employing the baseline setup in Kahn et al. (2021). Specifically, $\Delta_{i,t}^{\text{RCP26}} = 1 - y_{i,t}^{\text{RCP26}}/y_{i,t}^{\text{base}}$ and $\Delta_{i,t}^{\text{RCP85}} = 1 - y_{i,t}^{\text{RCP85}}/y_{i,t}^{\text{base}}$, where $y_{i,t}^{\text{RCP26}}$, $y_{i,t}^{\text{RCP85}}$, and $y_{i,t}^{\text{base}}$ are GDP per capita under RCP 2.6, RCP 8.5, and the baseline scenario, respectively. Thus from equation (6) we obtain $(\pi_{1,i}, \pi_{2,i})$ by solving the following minimization problem for each region i:

$$\min_{\pi_{1,i},\pi_{2,i}} \sum_{t=0}^{94} \left(\frac{1 + \pi_{1,i} T_t^{\text{RCP85}} + \pi_{2,i} \left(T_t^{\text{RCP85}}\right)^2}{1 + \pi_{1,i} T_t^{\text{RCP26}} + \pi_{2,i} \left(T_t^{\text{RCP26}}\right)^2} - \frac{1 - \Delta_{t,i}^{\text{RCP26}}}{1 - \Delta_{t,i}^{\text{RCP85}}} \right)^2 . \tag{A.1}$$

Here T_t^{RCP26} and T_t^{RCP85} are the global average temperature anomalies at time t (deviation from the pre-industrial temperature) under the RCP 2.6 and RCP 8.5 scenarios. Figure A.3 shows, with our calibrated climate damage coefficients, the ratios of GDP per capita between RCP 2.6 and RCP8.5 from our model, matches well with the ratios in Kahn et al. (2021).

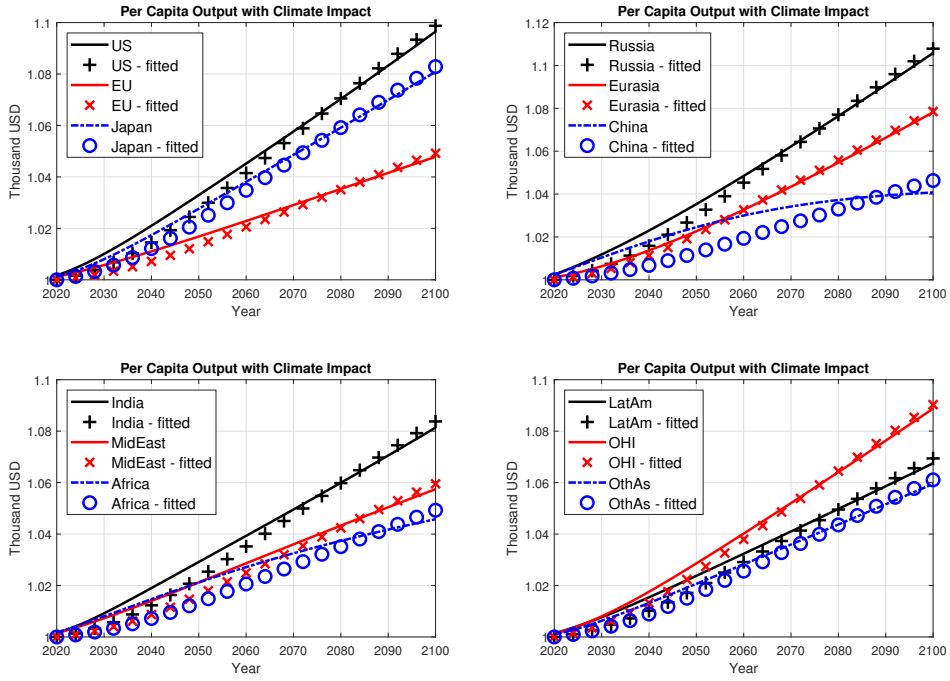

Figure A.4: Fitting climate damage parameters. Lines represent the ratios of GDP per capita between RCP 2.6 and RCP8.5 from Kahn et al. (2021); marks represent fitted ratios.

A.3.4 Regional Emission Cap Pathways

Figure A.5 displays the regional emission cap pathways, measured in Gigatonne of Carbon (GtC), for the baseline emission cap scenario, generated using the methodology described in Section 6.1.

Table A.6 lists the regional emission caps for every region in five-year time steps. The regional emission caps at annual time steps will be provided upon request.

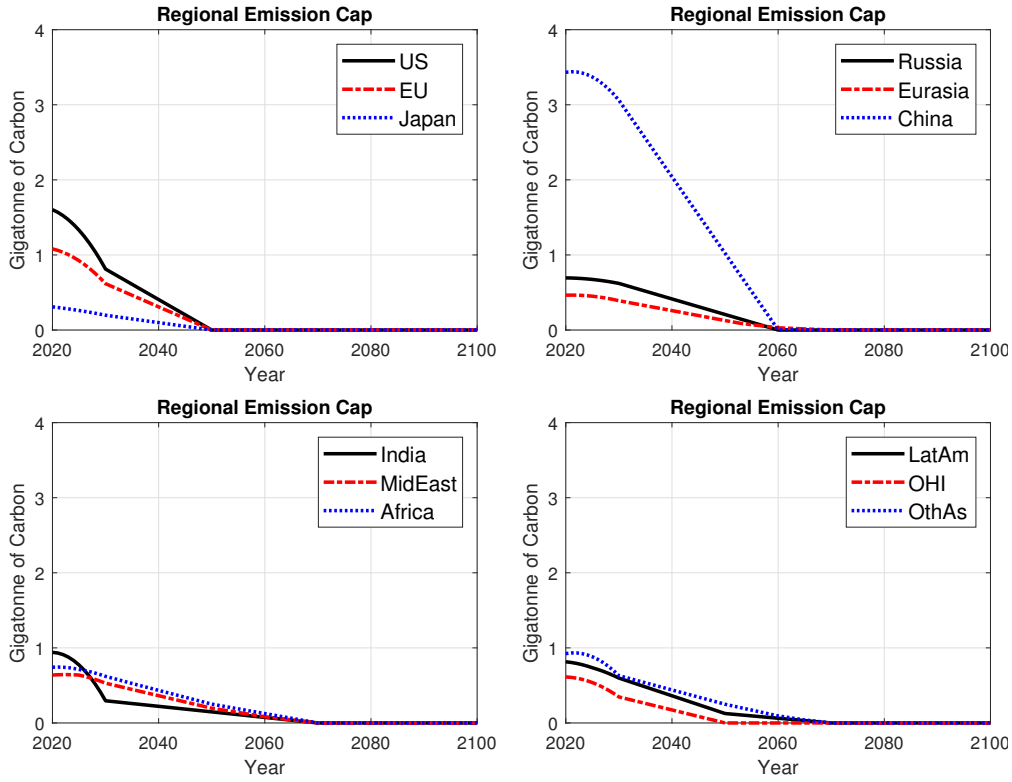

Figure A.5: Regional emission cap pathways under the baseline scenario.

Table A.6: Regional emission cap pathways under the baseline scenario (unit: GtC)

	2020	2025	2030	2035	2040	2045	2050	2055	2060	2065	2070
US	1.603	1.330	0.812	0.609	0.406	0.203	0.000	0.000	0.000	0.000	0.000
EU	1.081	0.923	0.617	0.463	0.309	0.154	0.000	0.000	0.000	0.000	0.000
Japan	0.308	0.260	0.197	0.148	0.099	0.049	0.000	0.000	0.000	0.000	0.000
Russia	0.694	0.674	0.621	0.517	0.414	0.310	0.207	0.103	0.000	0.000	0.000
Eurasia	0.464	0.450	0.390	0.324	0.259	0.193	0.126	0.071	0.030	0.015	0.000
China	3.433	3.370	3.061	2.551	2.042	1.532	1.023	0.513	0.004	0.002	0.000
India	0.940	0.773	0.295	0.259	0.222	0.185	0.148	0.111	0.074	0.037	0.000
MidEast	0.638	0.638	0.530	0.446	0.363	0.280	0.196	0.140	0.083	0.041	0.000
Africa	0.743	0.712	0.621	0.526	0.434	0.342	0.251	0.188	0.125	0.063	0.000
LatAm	0.815	0.736	0.598	0.480	0.362	0.244	0.126	0.094	0.063	0.031	0.000
OHI	0.613	0.538	0.347	0.260	0.173	0.087	0.000	0.000	0.000	0.000	0.000
OthAs	0.924	0.882	0.630	0.535	0.440	0.345	0.249	0.172	0.094	0.040	0.000

Figure A.6 presents a comparison of global emission cap pathways under various scenarios: the baseline scenario, net-zero by 2050, net-zero by 2070, and net-zero by 2090. In the net-zero scenarios, it is assumed that all countries achieve net-zero emissions by the respective target years.

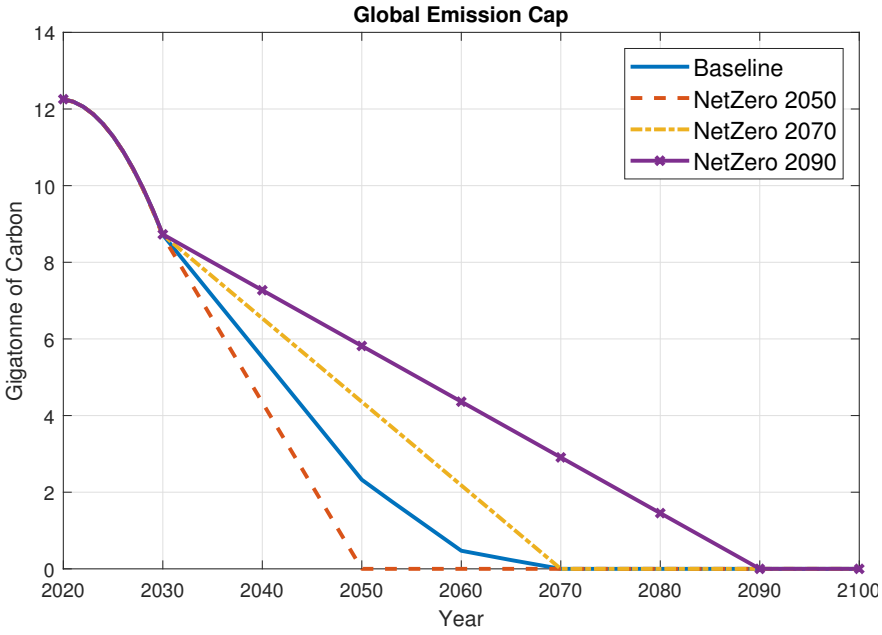

Figure A.6: Global emission cap pathways for the different net zero scenarios.

A.3.5 GDP Growth Rate beyond this Century

For the GDP growth rate beyond this century, we follow RICE to project $g_{t,i}$ for $t \geq 80$. We begin by assuming the long-run growth rate of TFP in the US is $g_{\text{US},\infty} = 0.0033(1-\alpha) = 0.00231$ with $\alpha = 0.3$. Next, we let $\widetilde{y}_{i,79} = y_{i,79}^{\text{BDD}} y_{i,0} / y_{i,0}^{\text{BDD}}$ be our projected per capita output in 2099, where $y_{i,0}$ is the observed per capita output in 2020. We then assume that the TFP growth in the US is characterized by

$$g_{\text{US},t} = g_{\text{US},\infty} + (g_{\text{US},79} - g_{\text{US},\infty}) \exp(-0.01(t-79)),$$

and let $\widetilde{y}_{\text{US},t+1} = \widetilde{y}_{\text{US},t} \exp(g_{\text{US},t}/(1-\alpha))$ for $t \geq 79$. For the regions other than the US, we assume their TFP growth can be expressed in relation to the TFP growth of the US. Specifically, we assume that, for $t \geq 79$,

$$\begin{cases} \widetilde{y}_{i,t+1} = \widetilde{y}_{i,t} \exp(g_{i,t}/(1-\alpha)) \\ g_{i,t+1} = g_{\text{US},t+1} + (1-\alpha)\chi \ln(\widetilde{y}_{\text{US},t}/\widetilde{y}_{i,t}) \end{cases}$$

where $\chi = 0.005$ is chosen such that $g_{i,t}$ gradually moves toward $g_{\text{US},t}$ as $t \to \infty$. [29]

[29] Assume $\widetilde{y}_{i,t} = A_{i,t} k_{i,t}^{\alpha}$ is GDP per capita where $k_{i,t}$ is capital per capita. We have

$$\ln\left(\frac{\widetilde{y}_{i,t+1}}{\widetilde{y}_{i,t}}\right) = g_{i,t} + \alpha \ln\left(\frac{k_{i,t+1}}{k_{i,t}}\right).$$

A.4 Additional Simulation Results

A.4.1 Benchmark Model: Regional Emissions

Figure A.7 displays the regional emissions under the noncooperative model with the ETS and the baseline emission cap scenario. Russia is the first to reach net zero emissions in 2050, followed by China and Latin America in 2056, MidEast in 2057, the US and Eurasia in 2058, and the OHI in 2059. Then, net zero emissions are achieved by EU in 2061, Japan and India in 2064. Finally, Africa and non-OECD Asia achieve net zero emissions in 2070.

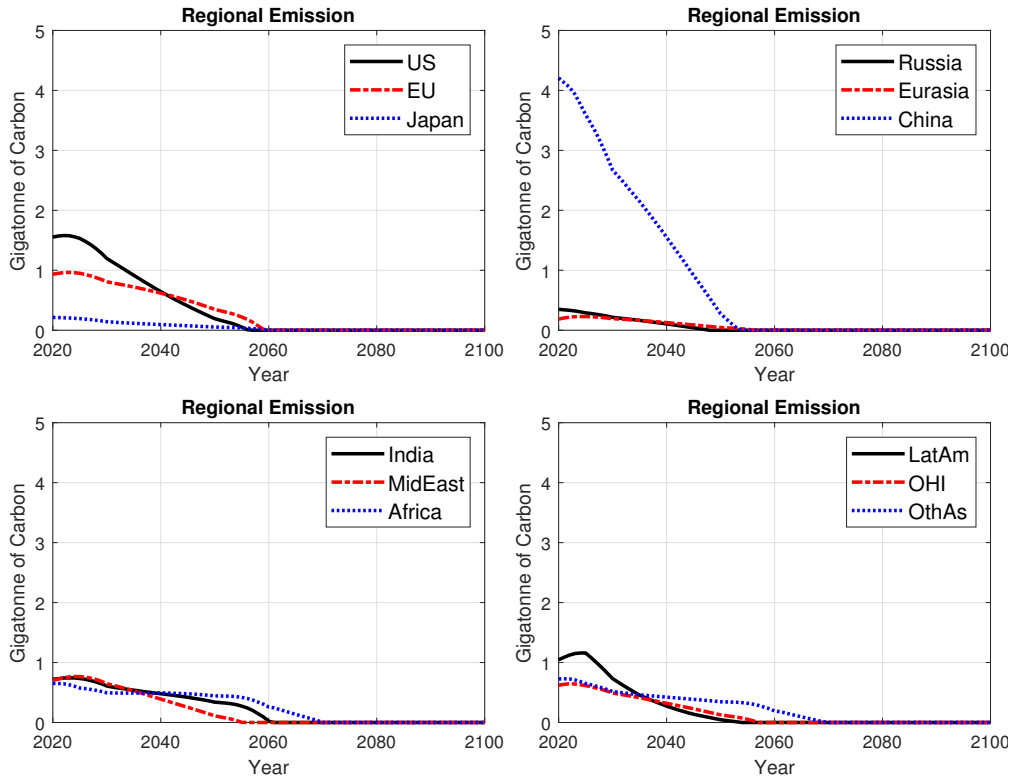

Figure A.7: Simulation results of regional emissions under the baseline emission caps.

If we assume the growth of $k_{t,i}$ is equal to the growth of GDP per capita, then we have

$$\widetilde{y}_{i,t+1} = \widetilde{y}_{i,t} \exp(g_{i,t}/(1-\alpha)).$$

A.4.2 Model Comparison of ETS Implementation

Figure A.8 compares regional net emissions between two cases under noncooperation with the baseline emission caps: (i) with the ETS, (ii) without the ETS.

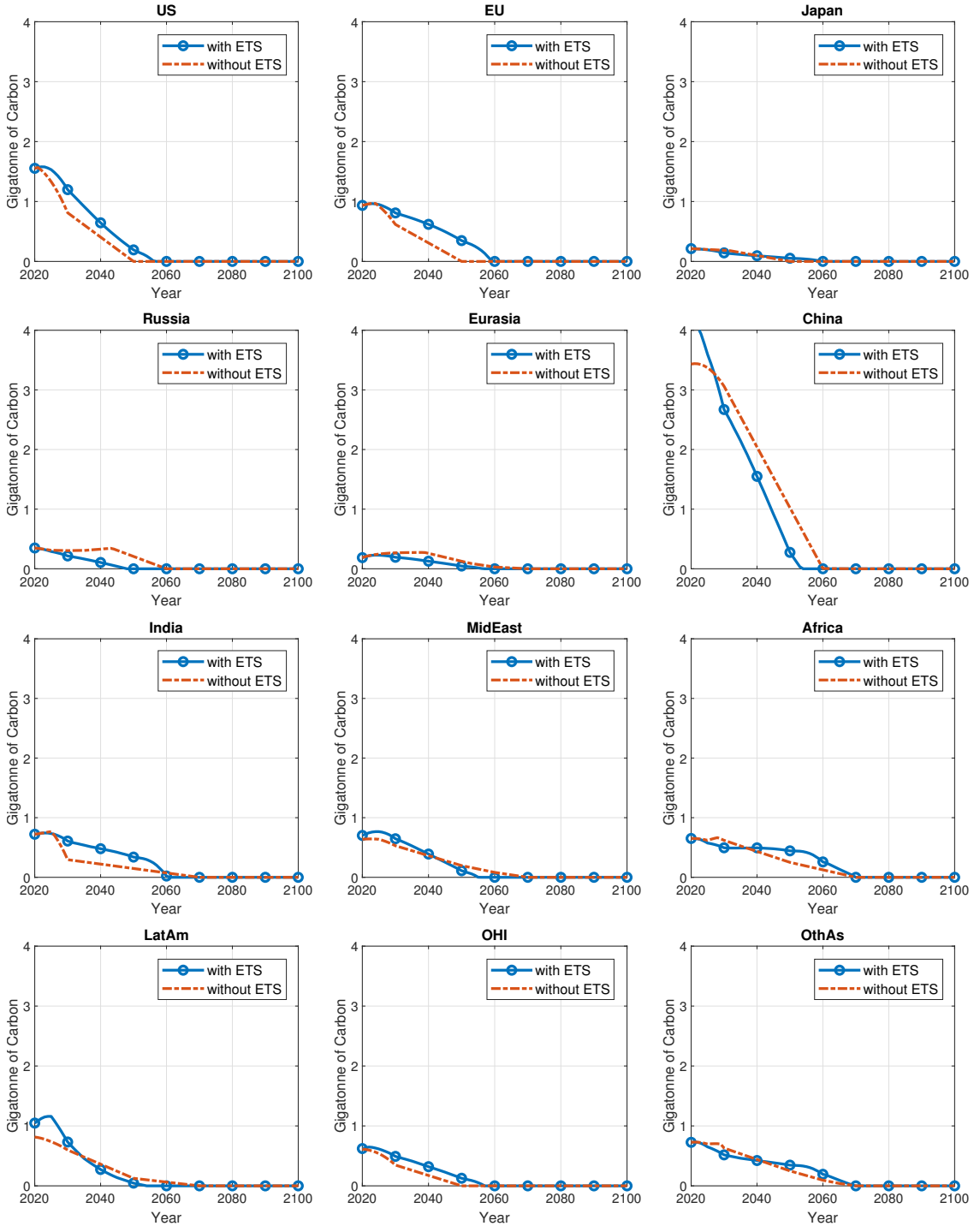

Figure A.8: Comparison of regional net emissions with and without the ETS.

Figure A.9 compares the regional MAC under noncooperation with the baseline emission caps. We compare two cases: (i) with the ETS, (ii) without the ETS.

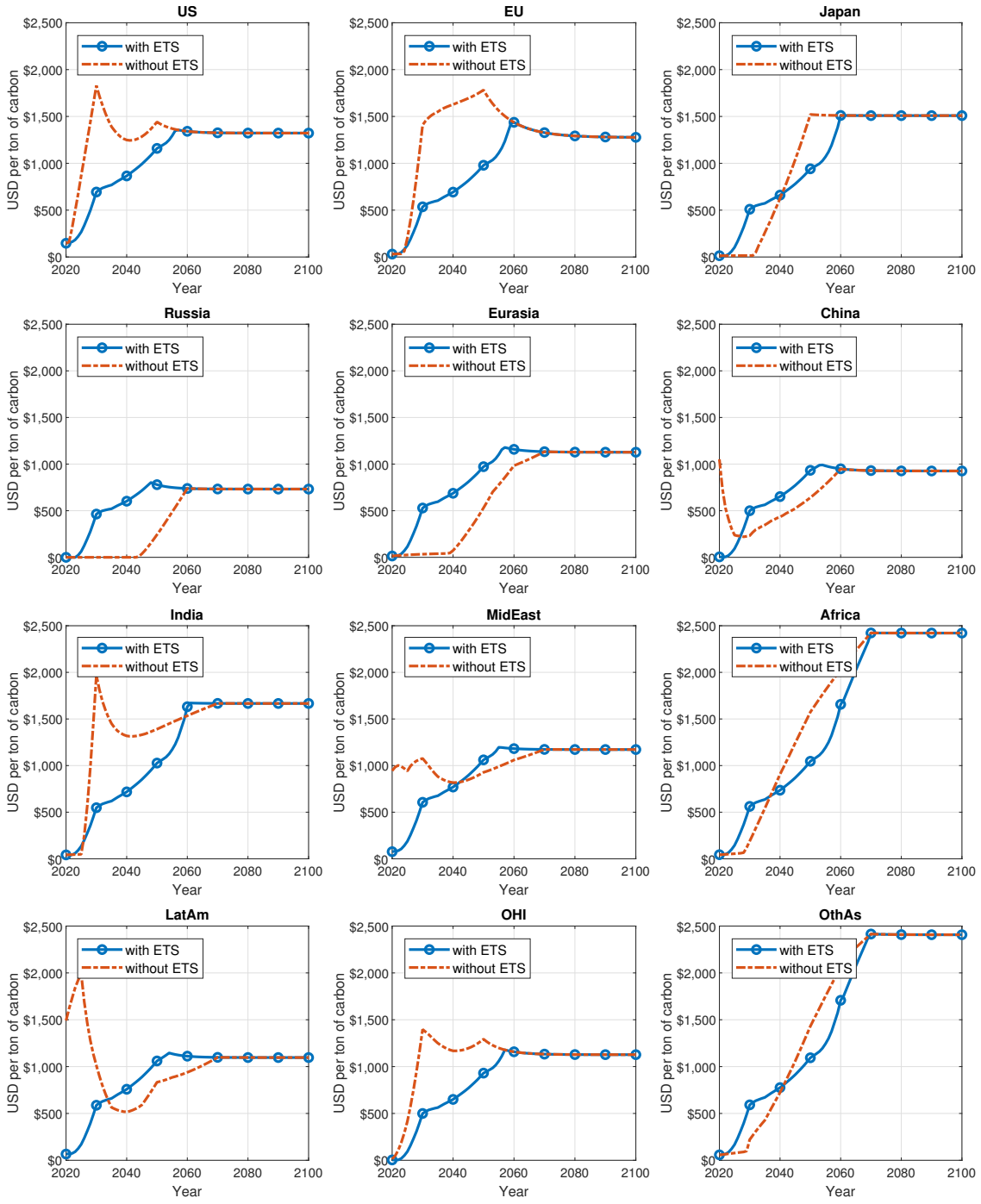

Figure A.9: Comparison of regional MAC with and without the ETS.

Figure A.10 compares the regional SCC under noncooperation with the baseline emission caps, comparing two cases: (i) with the ETS, (ii) without the ETS.

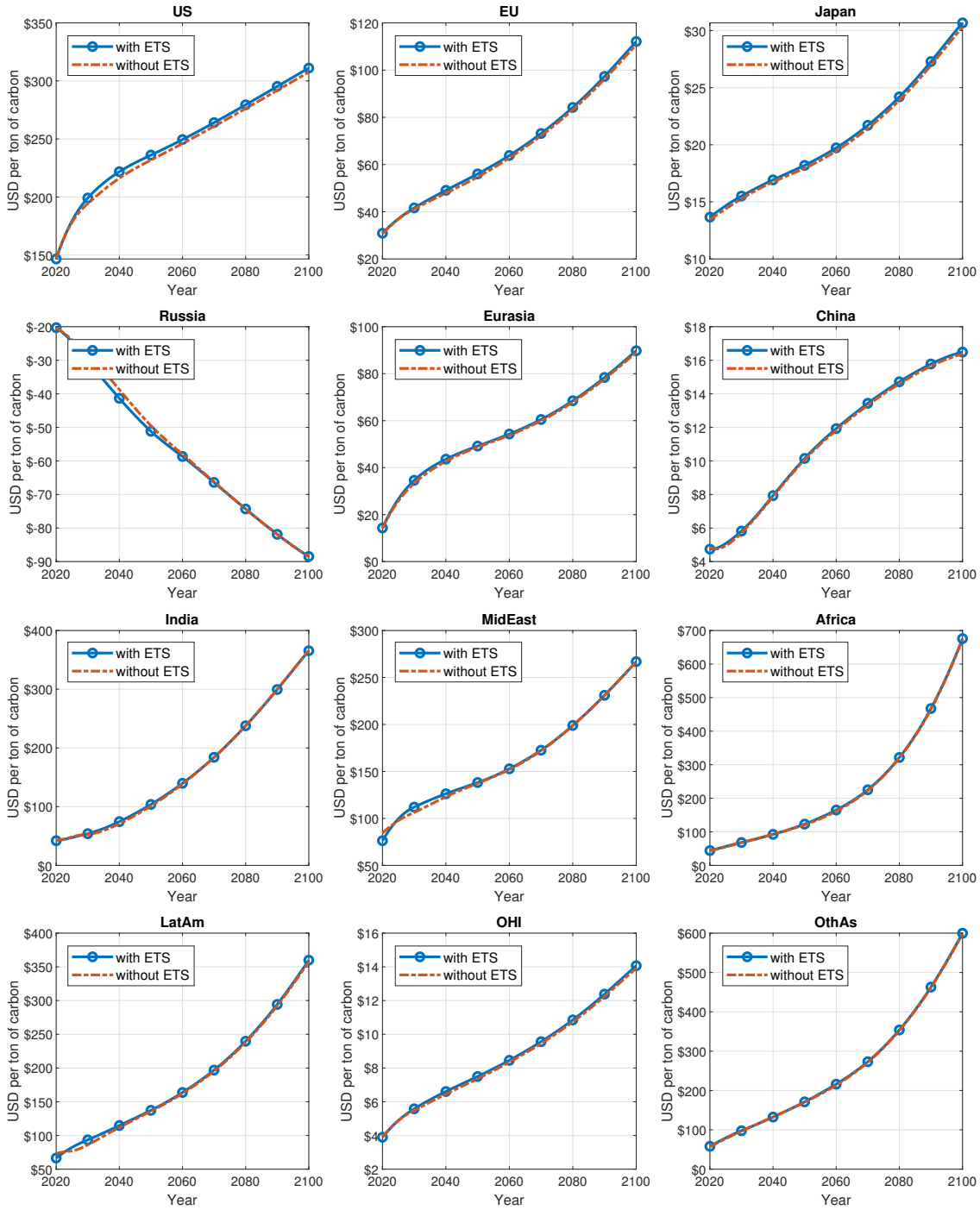

Figure A.10: Comparison of regional SCC with and without ETS.

A.4.3 Alternative Policy Simulations: Partial ETS

Figure A.11 compares the regional MAC under noncooperation, comparing two cases: (i) with the full ETS, (ii) with a partial ETS.

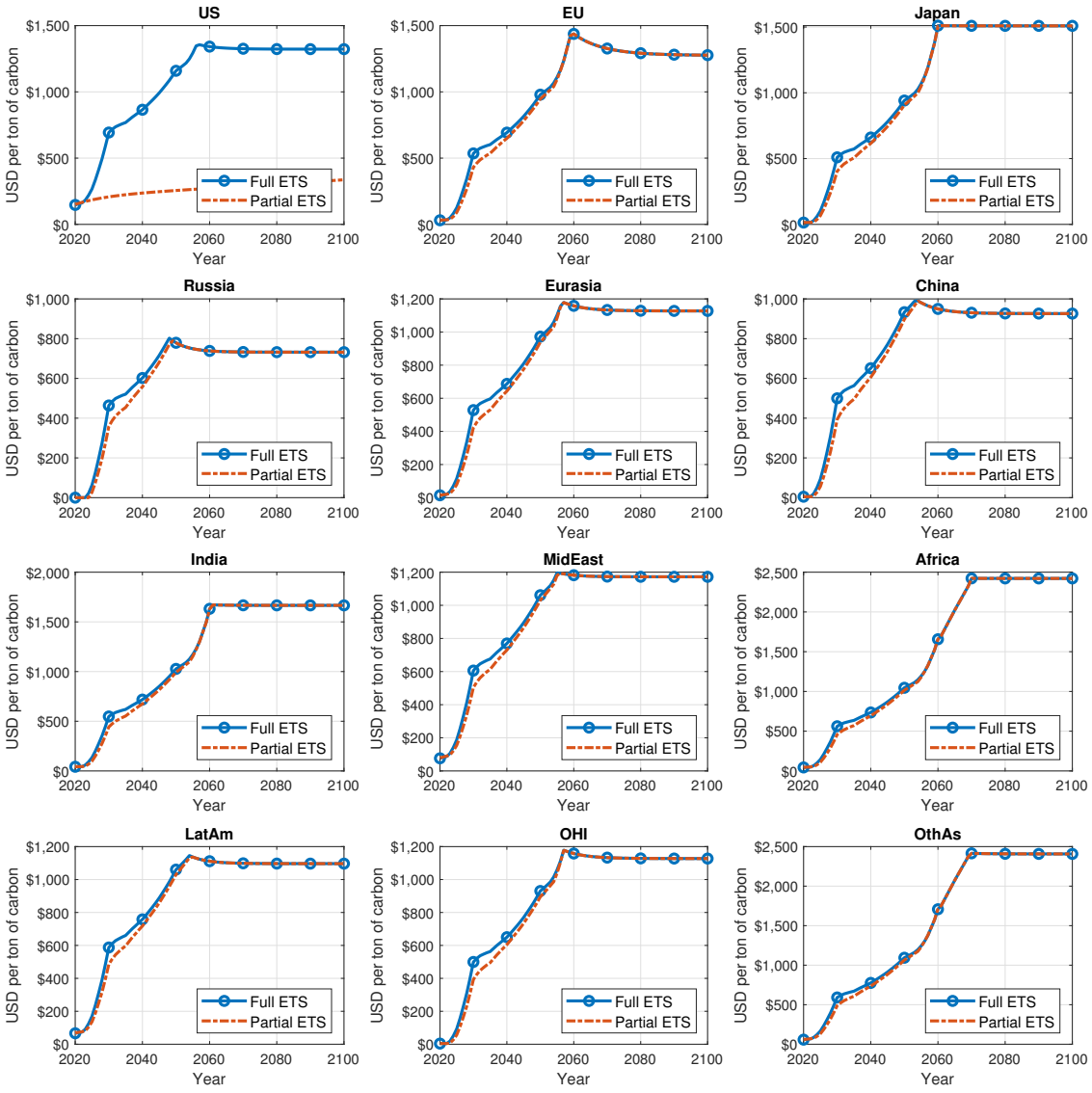

Figure A.11: Comparison of regional MAC under full and partial ETS scenarios.

Figure A.12 compares the regional SCC under noncooperation, comparing two cases: (i) with the full ETS, (ii) with the partial ETS without participation of the United States.

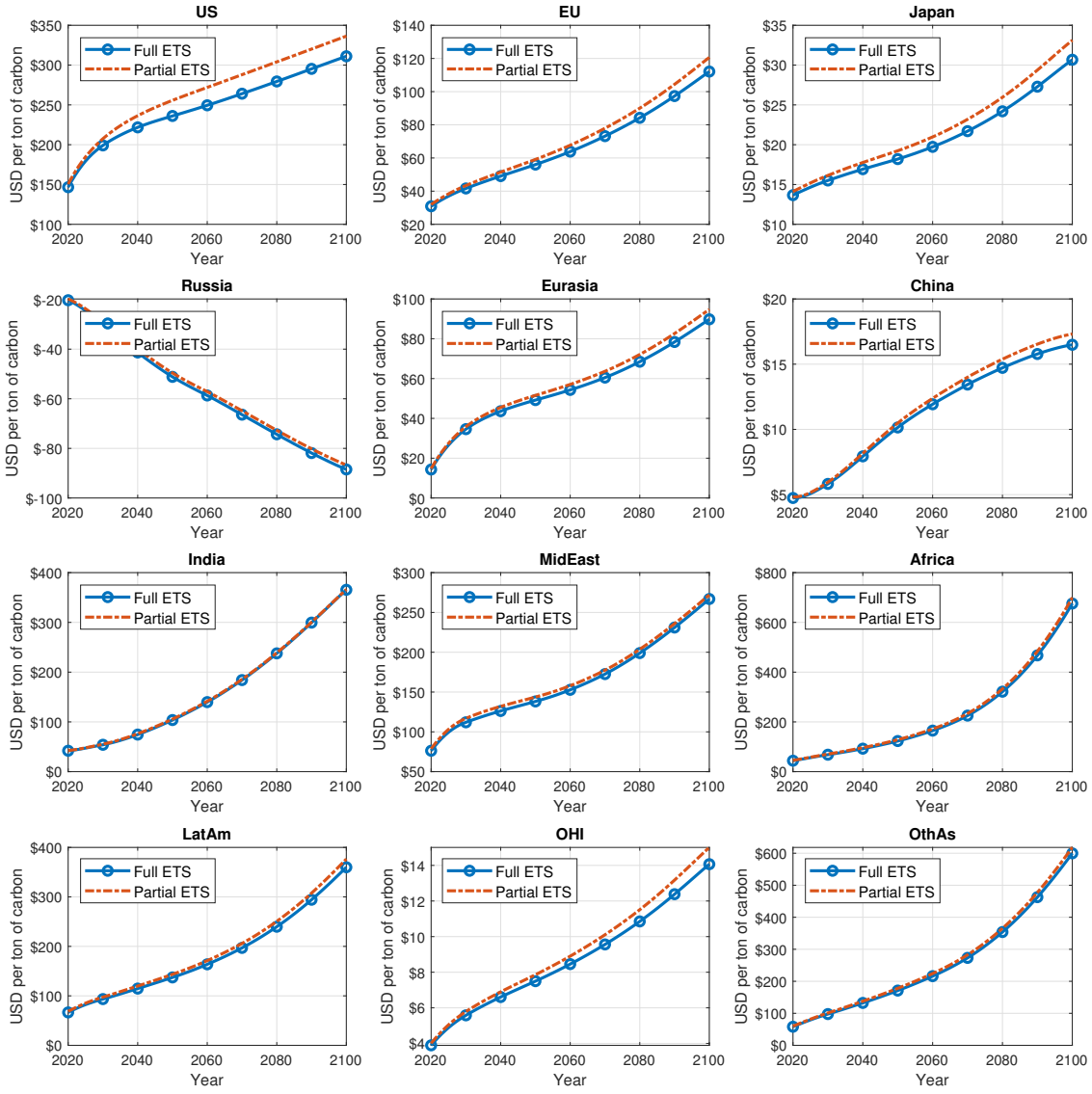

Figure A.12: Comparison of regional SCC under the full and the partial ETS scenarios.

A.4.4 Alternative Policy Simulations: Net Zero Scenarios

In Figure A.13, we compare the MAC for the noncooperative model with the ETS across alternative emission cap scenarios.

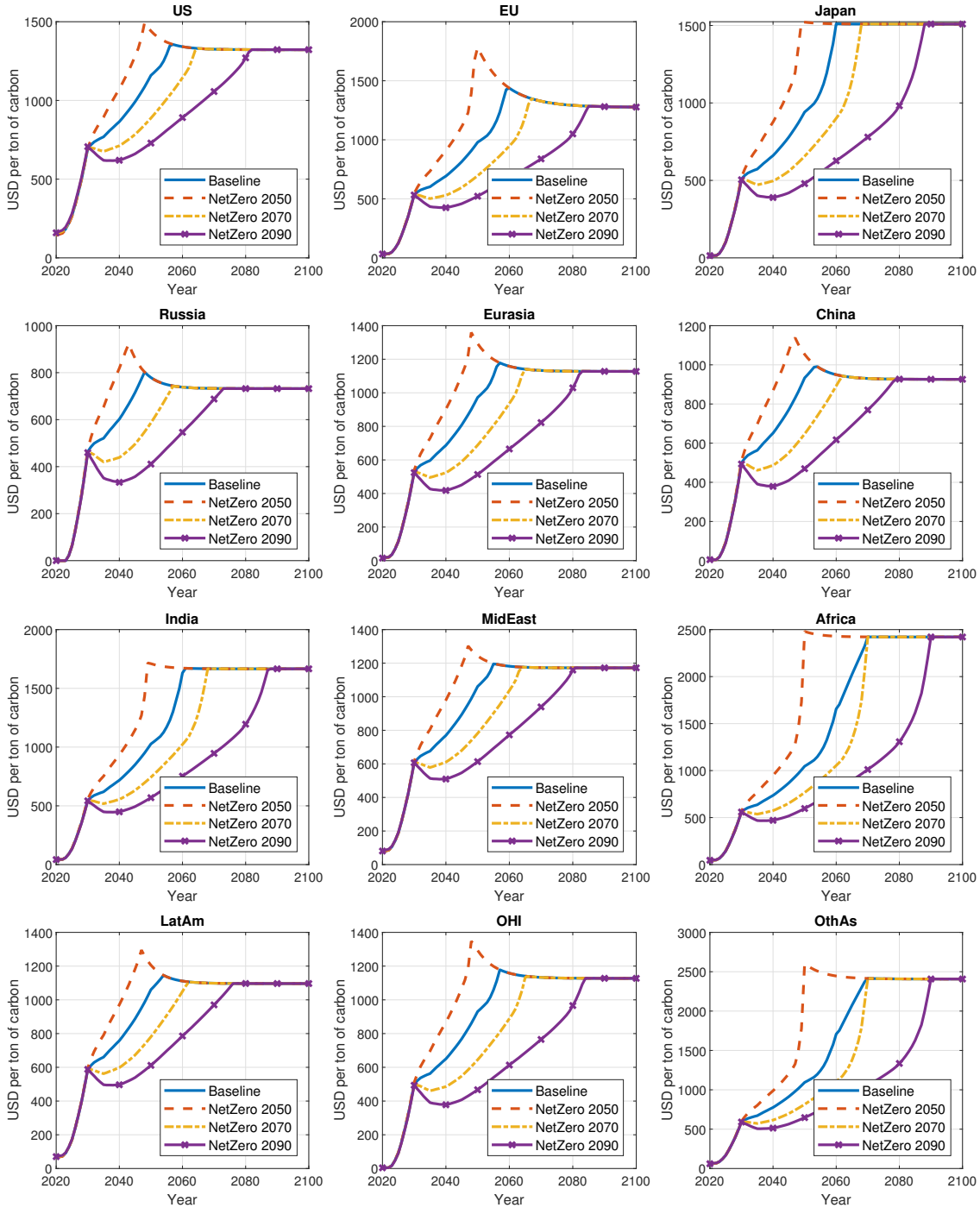

Figure A.13: Comparison of regional MAC under different emission caps.

Similarly, Figure A.14 displays the SCC of the noncooperative model with the ETS across different emission cap scenarios.

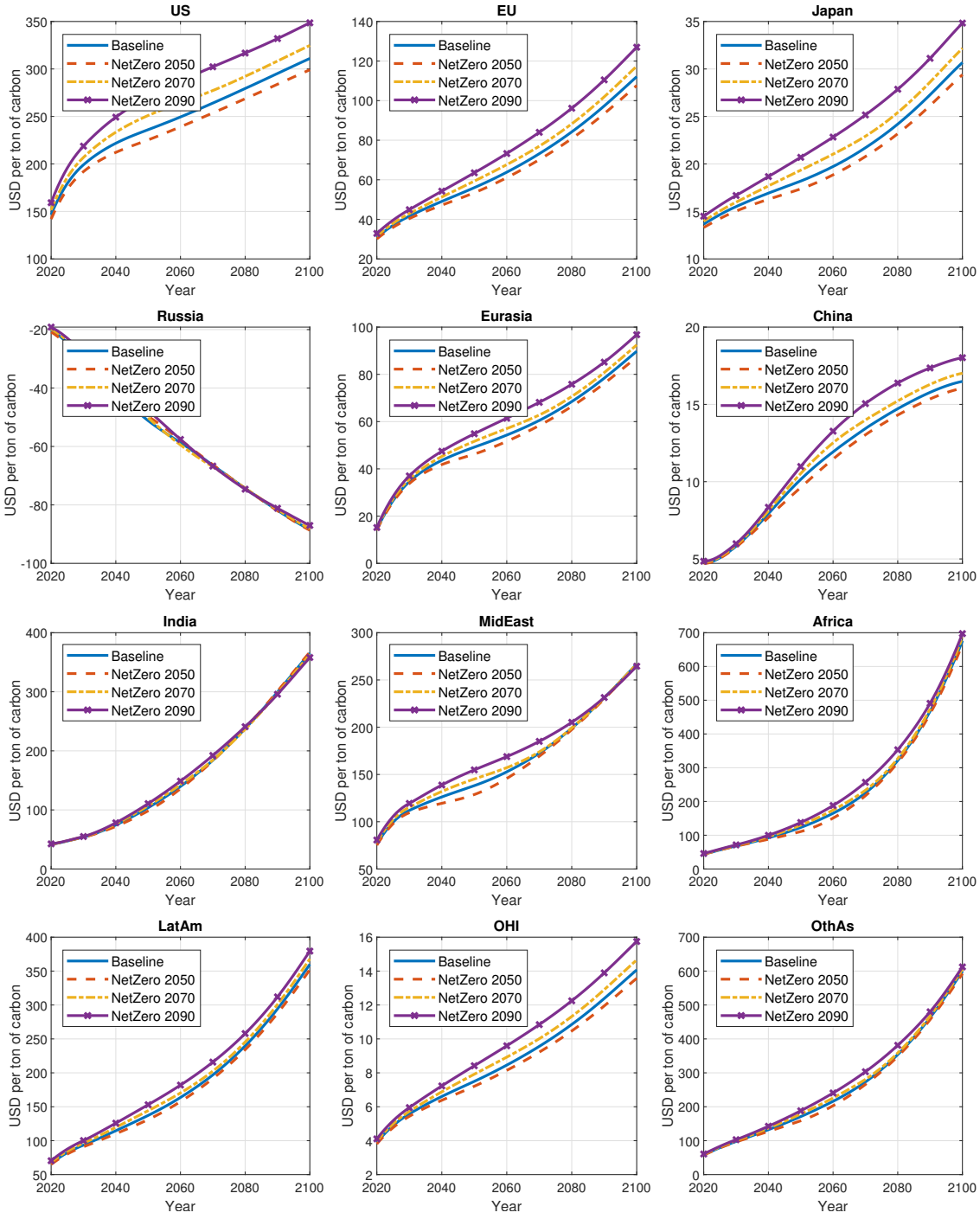

Figure A.14: Comparison of regional SCC under different emission caps.

A.4.5 Sensitivity Analysis over Climate Damage Parameters

In Figure A.15, we compare the MAC for the noncooperative model with the ETS under alternative climate damage parameters ($\pi_{1,i}$, $\pi_{2,i}$), based on projections from Kahn et al. (2021) and Nordhaus (2010a) alongside the baseline projection from Burke et al. (2018).

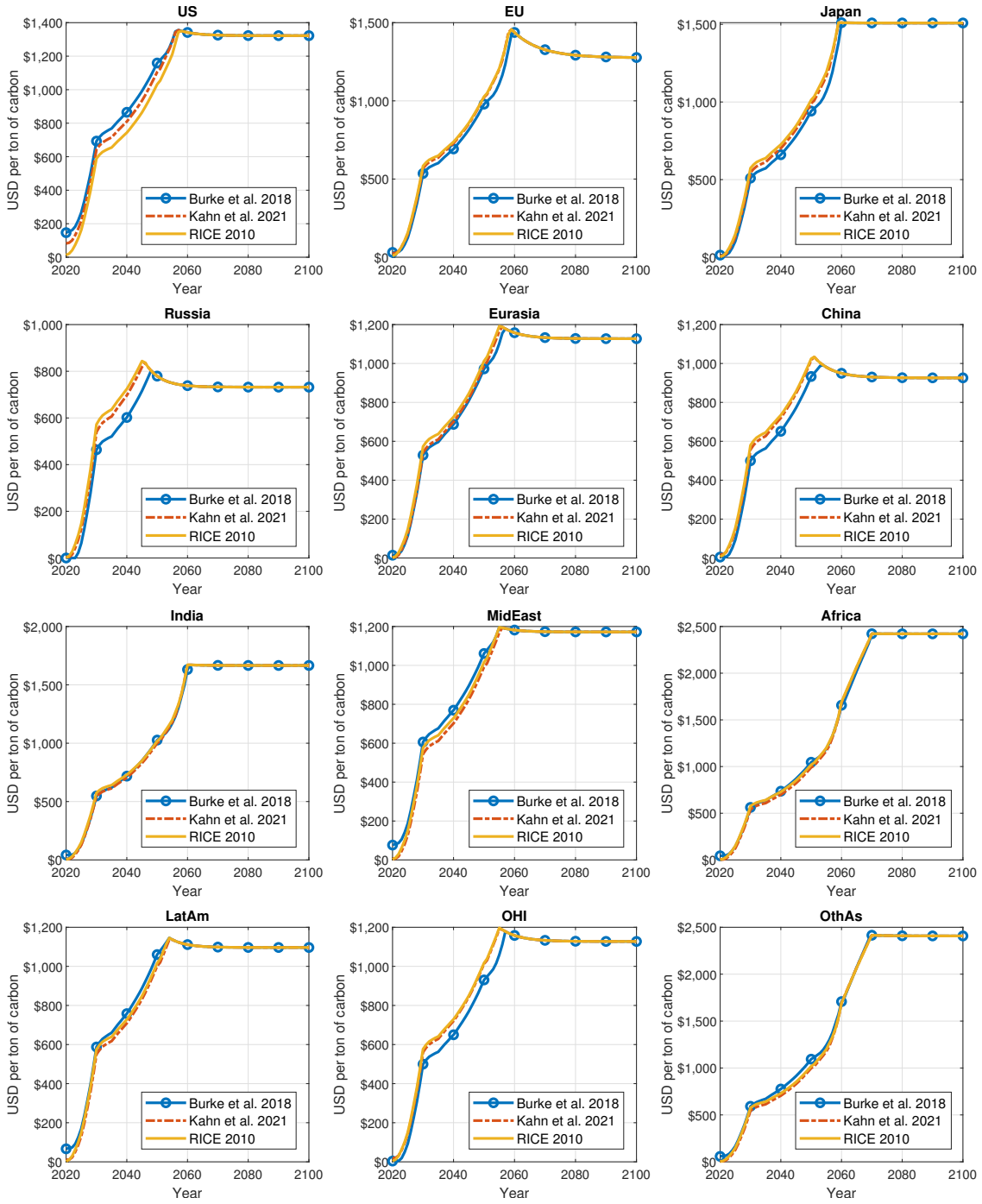

Figure A.15: Comparison of regional MAC under different estimates of climate damages.

Similarly, Figure A.16 displays the SCC of the noncooperative model with the ETS under different values of the climate damage parameters.

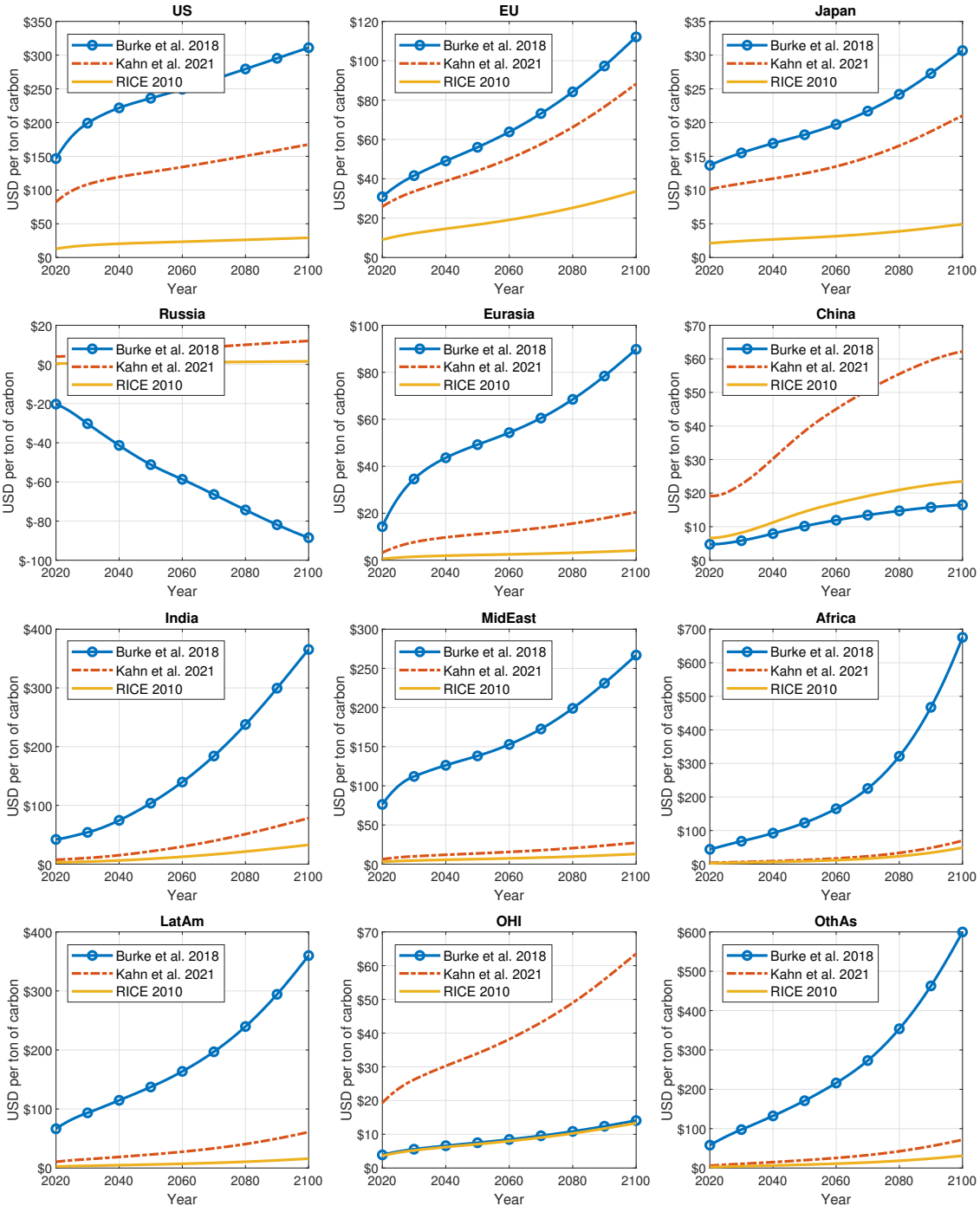

Figure A.16: Comparison of regional SCC under different estimates of climate damages.

A.4.6 Sensitivity Analysis over Abatement Cost Parameters

In Figure A.17, we compare the MAC for the noncooperative model with the ETS under alternative estimates of the emissions abatement parameters ($b_{1,i}$, $b_{2,i}$, $b_{3,i}$, $b_{4,i}$), calibrated from Ueckerdt et al. (2019) and Nordhaus (2010a).

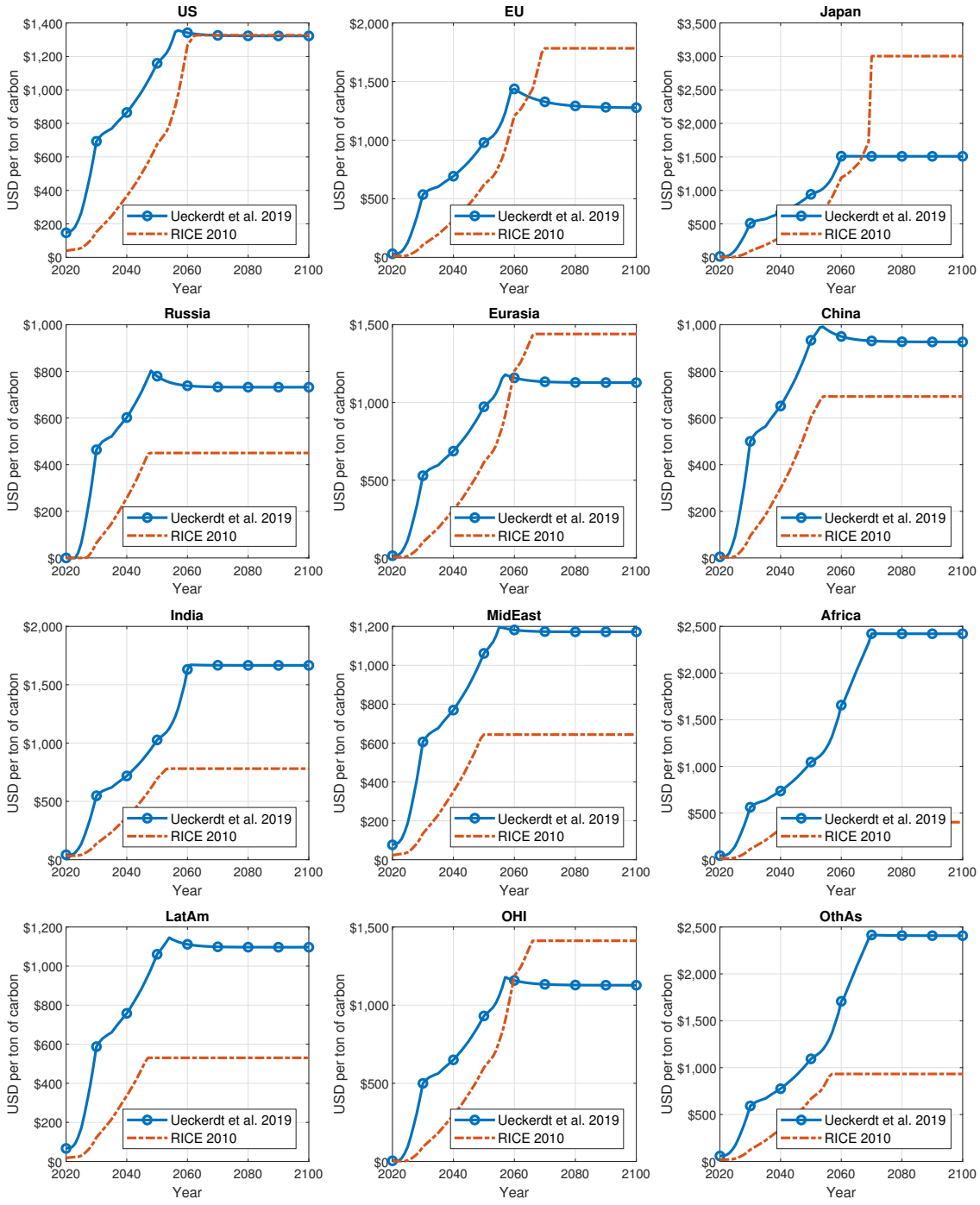

Figure A.17: Comparison of regional MAC under different estimates of emissions abatement cost.

Similarly, Figure A.18 displays the SCC of the noncooperative model with the ETS under different emissions abatement cost estimates.

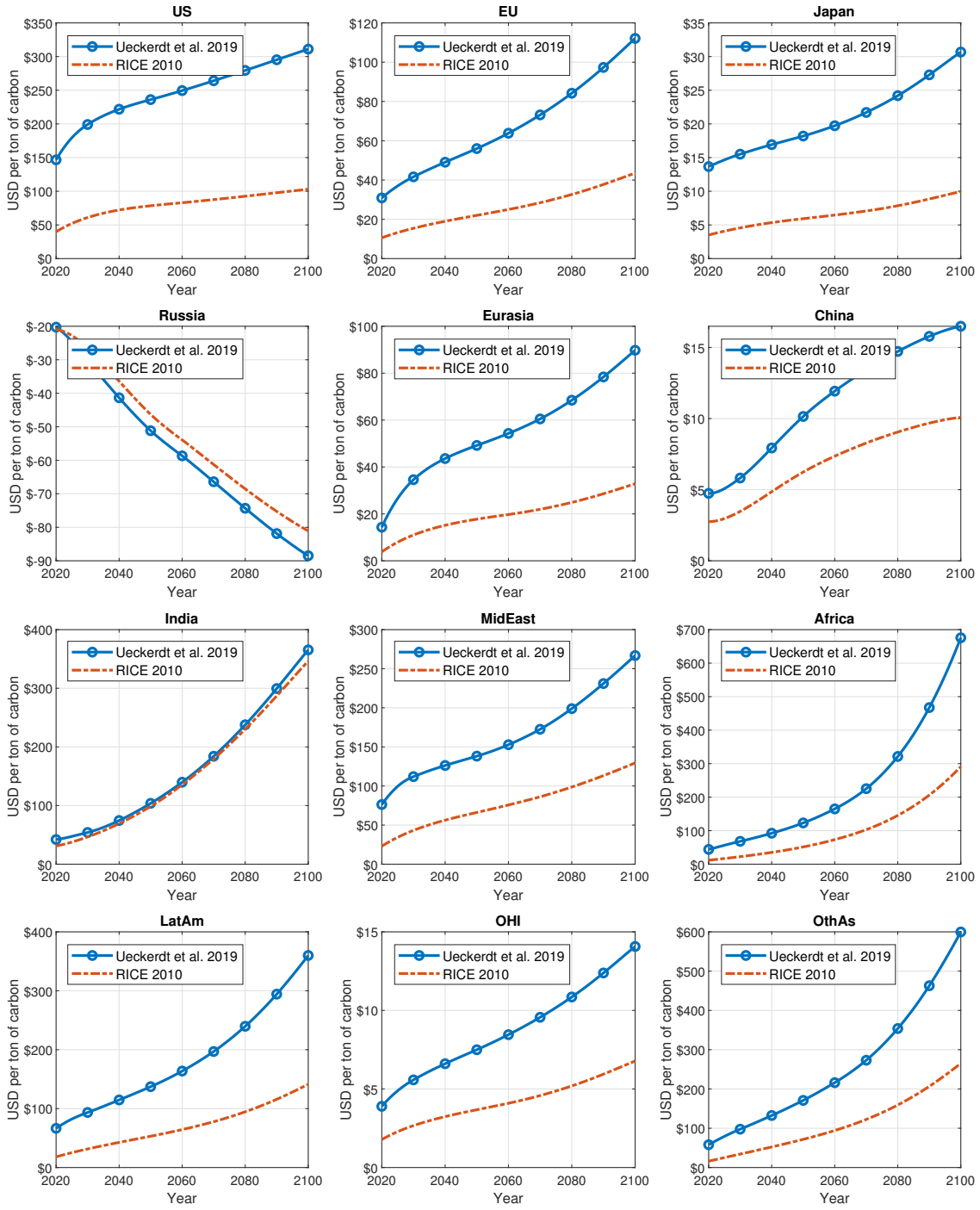

Figure A.18: Comparison of of regional SCC under different estimates of emissions abatement cost.

A.4.7 Sensitivity over TFP Growth Rates

Figure A.19 compares key model outcomes under different TFP growth rates: the baseline TFP growth rates derived from Burke et al. (2018) and the alternative rates based on Nordhaus (2010a).

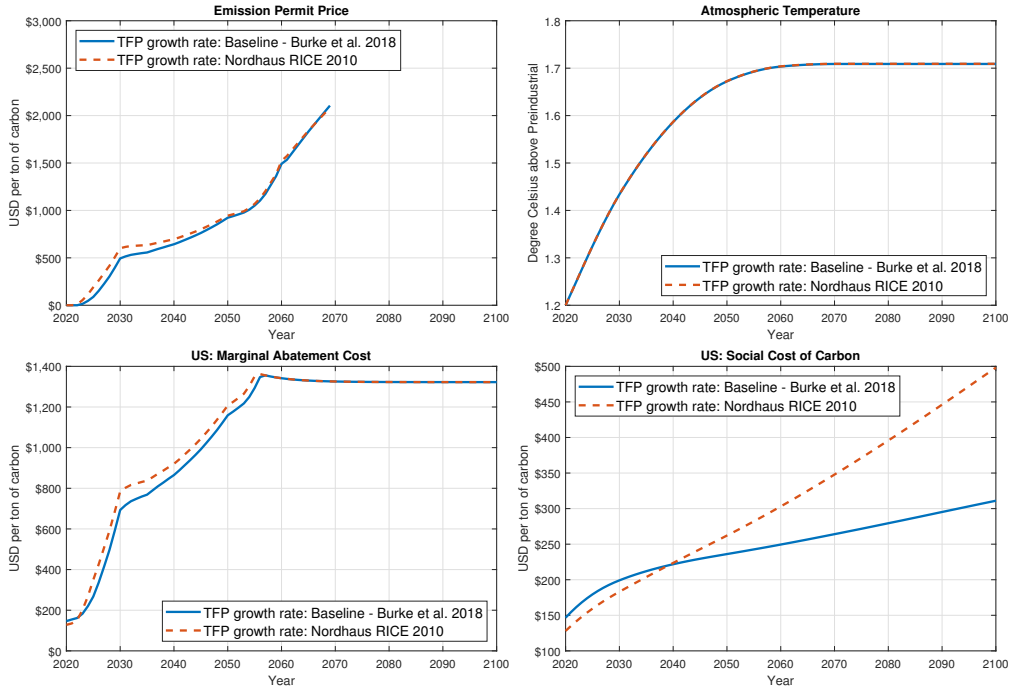

Figure A.19: Comparison of simulation results under different TFP growth rates.